www.dergipark.gov.tr
ISSN:2148-3736
El-Cezerî Fen ve Mühendislik Dergisi
Cilt: 6, No: 3, 2019 (428-457)

El-Cezerî Journal of Science and Engineering
Vol: 6, No: 3, 2019 (428-457)
DOI:10.31202/ecjse.547060

ECJSE

Research Paper / Makale

Chalcogenide Glasses

Bekir KARASU, Tuğçegül İDİNAK, Eda ERKOL, Ali Ozan YANAR

Eskişehir Technical University, Engineering Faculty, Department of Materials Science and Engineering, 26555, Eskişehir TÜRKİYE
bkarasu@eskisehir.edu.tr

Received/Geliş: 30.03.2019 **Accepted/Kabul:** 14.06.2019

Abstract: Chalcogenide glasses, which are among the technologically very important materials, contain at least one chalcogen element as a major constituent and their utilization ranges from infrared (IR) optics applications to phase–change, optical–electrical data–recording. The interest to spectacle glasses exhibiting transparency in the IR region of the optical spectrum coincides with the mid–twentieth century. Firstly, heavy metal oxides were investigated and the transparency limit was extended from 3–5 µm (classical oxide glasses) to 7–8 µm wavelength. The widespread usage of infrared optics in the 20th century has led to the need for new IR materials and to increase the IR transparency limit over 8 µm and scientists have tried chemical compositions of S, Se and Te in the 6th group of the periodic table. Compared to oxide glasses, their mechanical strength and thermal stability are considerably lower and the calorimetric glasses form a new glass group with semiconductor properties. In this article, a brief overview of the definition, historical development, structure, properties and potential applications of chalcogenide glasses dating back to the early 1950s is given.

Keywords: Chalcogenide glass; history; property; application

Kalgojenit Camlar

Öz: Teknolojik olarak çok önemli malzemeler arasında yer alan kalkojenit camlar, ana bileşen olarak en az bir kalkojen element içeren, kullanımları kızıl–ötesi (İnfra–red, IR) optik uygulamalardan faz değişimi, optik–elektriksel veri kaydına kadar değişmektedir. Optik spektrumun kızılötesi bölgesinde şeffaflık sergileyen gözlüklere olan ilgi 20. yüzyılın ortalarına denk gelmektedir. İlk olarak, ağır metal oksitler araştırılmış ve saydamlık sınırı 3–5 µm'den (klasik oksit camları) 7–8 µm dalga boyuna kadar uzatılmıştır. 20. yüzyılda, kızıl–ötesi optiklerin yaygın kullanımı, yeni IR malzemelerine ihtiyaç duyulmasına ve IR şeffaflık sınırının 8 µm'nin üzerine çıkmasına yol açmış ve bilim insanları periyodik cetvelin altıncı grubundaki S, Se ve Te'ün kimyasal bileşimlerini denemişlerdir. Oksit camlara kıyasla, daha düşük mekanik mukavemet ve ısıl kararlılığa sahip kalorimetrik camlar yarı iletken özellikleriyle yeni bir cam grubunu oluşturmaktadırlar. Bu makalede, geçmişleri 1950'lerin başlarına kadar uzanan kalgojenit camların tanımı, tarihsel gelişimi, yapısı, özellikleri ve potansiyel uygulamalarına yer verilmiştir.

Anahtar kelimeler: Kalgojenit cam; tarihçe; özellik; uygulama

1. Introduction

1.1. Chalcogens

Chalcogen's elements can be found in 6th group (or VI) of the periodic table, consists of O, S, Se, Te, and Po (Fig. 1). Blitz & Fischer proposed the group's name in 1932 [1]. **"Chalcogens"** has been driven from the Greek word chalcos (**ore formers**). **"Chalcogenides (Ch)"** referring to their compounds have metallic character. O and S are non–metals, unlike Se and Te being metalloids and Po is a metal.

How to cite this article
Karasu, B.,, İdinak, T., Erkol, E., Yanar, A. O., *"Chalcogenide Glasses"* El-Cezerî Journal of Science and Engineering, 2019, 6.(3); 428-457.

How to cite this article
Karasu, B.,, İdinak, T., Erkol, E., Yanar, A. O., *"Kalgojenit Camlar"* El-Cezerî Fen ve Mühendislik Dergisi 2019, 6(3); 428-457.

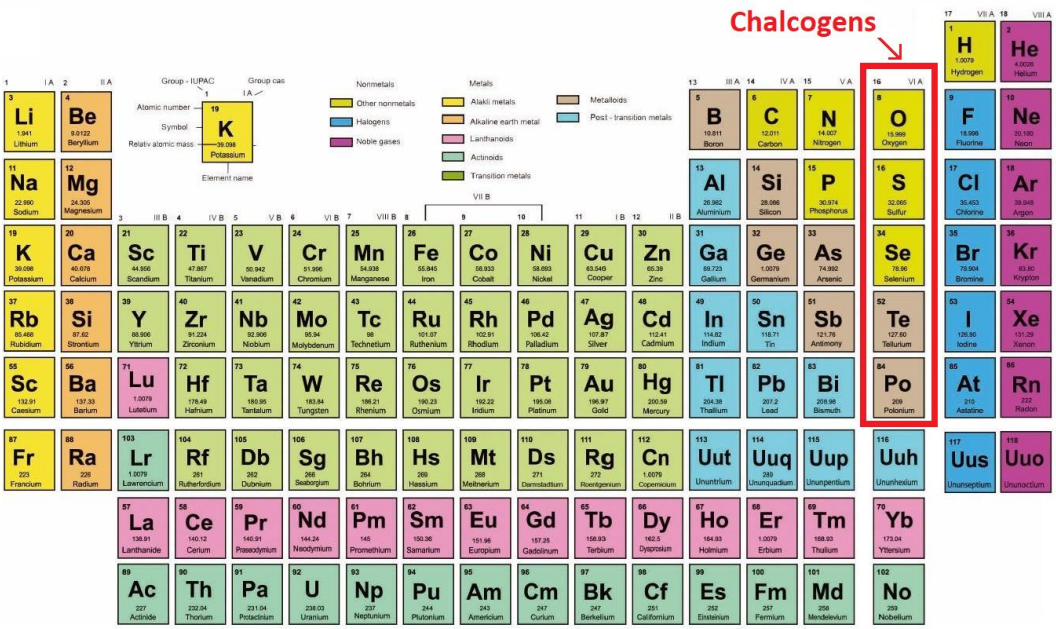

Figure 1. Chalcogens in the periodic table [2]

1.2. Chalcogenide Glass (ChGs)

ChGs could be produced by mixing the chalcogen elements, such as S, Se and Te with Ga, In, Si, Ge, Sn, As, Sb, and Bi, Ag, Cd, Zn etc., belonging to an important class of amorphous solids, indicating a short–or medium–range order molecular structure. Glass, being an amorphous and isotropic material, can also be defined as an inorganic fusion product cooled down to a rigid form without any crystallization. Similar to all other glasses ChGs inhibit a glass transition temperature (T_g), being quite important for converting bulk glasses into the forms of thin film and fibre.

ChGs possess several extra ordinary properties making them interesting materials when compared to other kinds, especially for the opto–electronic applications.

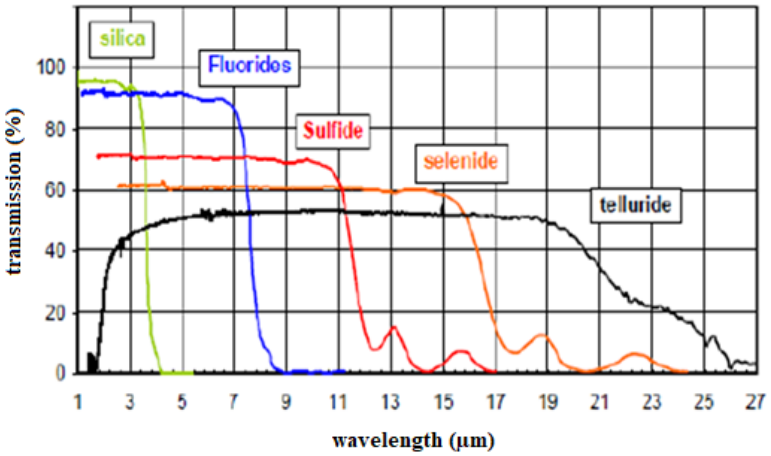

Figure 2. Comparison of the optical transmission of ChGs with silica and fluoride glasses [3]

Their properties of high infra–red transparency (Fig. 2), high refractive index, photo–sensitivity, alloying and doping capability, low–phonon energy and suitability to low–temperature processing lead them to be intelligent materials for the optical integration application. Fig. 3 indicates the characterization of ChGs as glasses and semiconductors with other materials.

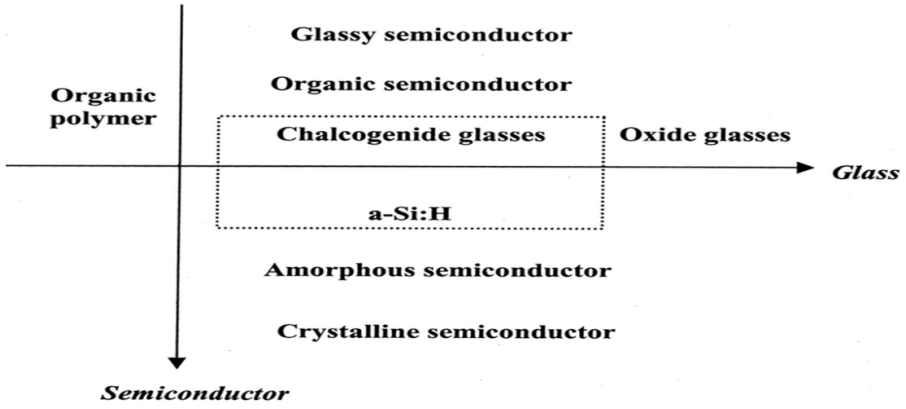

Figure 3. Characterization of ChGs as glasses and semiconductors with other materials [4]

2. History

The earliest experimental data on non oxygen–containing glass were reported by Schulz–Sellack in 1870 [5]. Followingly, Wood (1902) [6], and Meier (1910) [7] carried out the first researches on the optical properties of vitreous Se.

The deal with glasses showing transparency in the IR region coincides with mid–20th century. Firstly, the heavy metal oxides were investigated, and the transparency limitation was enlarged from 3–5 μm (the case of the classical oxide glasses) to 7–8 μm wavelength. To prolong such a limit further, the researchers made an effort on the chemical compositions based upon the sixth group's elements in the periodic table, the chalcogens: S, Se and Te.

The first work on ChGs was attributed to Frerichs in the early 50's on As_2S_3 glass and the paper with the title of: "New optical glasses transparent in IR up to 12 μm" was published [8–9] and As_2S_3 by Fraser [10] and Dewulf [11]. Frerichs was also at the investigation of development of Se glasses and binary compounds with sulphur. Another scientist of vitreous ChG around that time was Winter–Klein [12]. The major research on ChG was started by two research groups from Saint–Petersburg; one team was led by Kolomiets and Goryunova who reported to discover the first semiconducting glass [13] based on halogen elements while the older group was led by Myuller. In 1968, Ovshinsky found memory and switching effects in ChG [14–15]. This led to the development of non–crystalline ChGs in various field such as xerography or computer memories. Around the same time Sir Mott (Nobel Prize winner in Physics in 1977) and Davis developed the theory on the electronic processes in ChG [16]. After that, several review books were published in subsequent years on glasses by Zallen in 1983 and by Elliott. However, the first review book entirely dedicated to Ch materials, "Glassy semiconductors", was published in 1981 by Borisova. Andriesh published a book entitled "Glassy semiconductors in photo–electric system for optical recording of information" on ChG with special dedication to their applications in 1988. In 2000, Popescu gave a detailed account on the physical and technological aspect of Ch system in his book, "Non–crystalline chalcogenides", which is the most detailed book published to date in the field of amorphous and glassy Ch materials. The book covers the scientific and technological information on chalcogens (S, Se and Te) and Ch combinations [17–19].

3. Compounds of ChGs

3.1. Binary Ch

Numerous number of studies on the structure of ChGs have been conducted in binary compositions taking the forms of both bulk and thin film into an account. Chalcogens could form alloys together,

Se–S [20], Se–Te [21] and S–Te glassy [22–23] compounds were identified for different compositions by varying one or the other chalcogen. Among the most interesting elements, antimony (Sb), copper (Cu), germanium (Ge), phosphorus (P), arsenic (As), silicon (Si) and tin (Sn) are considered good network formers with chalcogen elements. Binary mixtures of Ge and As with Se are most commonly studied because they have large glass forming regions. Abrikosov and his co–workers [24] reported the phase diagram for the As–S and As–Se systems, the existence of As_2S_2 and As_2S_3 compound for the first system and AsSe and As_2S_3 for the second system. The first phase diagram for Ge–Se system has been examined by thermal and x–ray phase analysis [25]. Glass formation in Ge–Se system takes predominant place in alloys enriched with Se, containing 0 to 25 at % of Ge [26]. Tronc et al. [27] achieved the glasses in the Ge_xSe_{1-x} ($0 \leq x \leq 0.4$) system (from elemental Se to $GeSe_{1.5}$).

3.2. Ternary Ch

In chalcogen system, glass formation region is comparingly narrow [28]. Incorporation of As, Ge and few other polyvalent elements into chalcogens contribute to reasonable stabilization of their structure. When the number of components is increased this tends to widen the glass forming region and ternary glasses have been formed with components from every column of periodic table. There are many 3 components (ternary) chalcogenide systems which form glasses over a wide range such as As–Se–Ge [29–32], Ge–Se–Te [18, 33], As–S–Se [34–35], As–Se–Te [36], As–Se-In [37], Ge–Se–In [38] etc.

3.3. Metallic Additives in ChGs

It was thought for a long time that amorphous semiconductors could not be doped because of the following two reasons:

- Any foreign atom introduced into an amorphous matrix would take up its normal chemical valence because of supposed flexibility of the random network which is conductive to satisfy the local coordination.
- The density of states in the gap is sufficiently large so that the Fermi level does not shift by the addition of electrons and holes supplied by impurity atom.

The possibility of doping these materials was first demonstrated [39–40] in amorphous hydrogenated Si; for doping with hydrogen, a large impurity concentration was required [41–42]. In these studies, the term “modifier” or “additive” is used for metal atoms introduced. Comparing to conventional dopants in crystalline semiconductors (in which one is considering dopant material in ppm) the modifiers or additives are in much larger amounts ranging from a few atomic % to sometime as high as 20 to 30 at. %.

On metallic addition interesting effects observed in ChGs are:

- Chemical modification of several chalcogenide glasses by introduction of large quantity of certain metals,
- Transformation in the type of electronic conductivity from the generally observed p– to n–type on the incorporation of metals as Bi, Pb etc.,
- In general, the addition of metal in multi–component glasses can affect their spatial, structural, chemical, electronic and optical properties. These effects can be therefore being probed not only by studying the electrical conductivity but by a careful characterization and analysis of other properties as well.

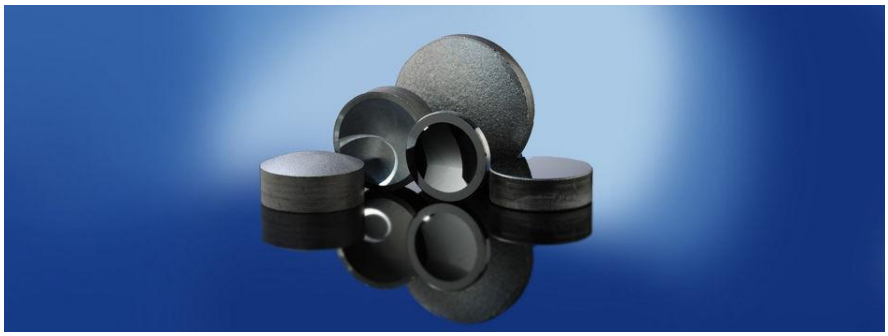

Figure 4. Infrared ChG [43]

4. Structure and Chemical Bonding of ChGs

The perfect periodicity in space cannot be seen in a real crystal which has varying sorts of imperfections or defects. Solids lacking the atomic regularity are named non–crystalline solids or amorphous, vitreous or glassy solids. However, the 1st and 2nd nearest–neighbour coordination shells are well–described, atoms in the 3rd coordination sphere become un–correlated with those in the first one. It is difficult to define an ideal non–crystalline skeleton. Especially, different thermal treatments result in various non–crystalline atomic arrangements. A continual random network [44] may be thought to be an ideal non–crystalline skeleton for covalently bonded solids.

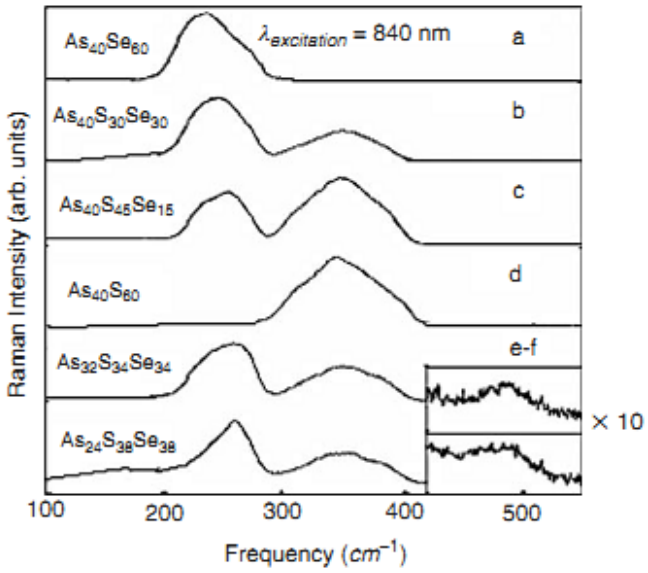

Figure 5. Raman intensity versus frequency relationship of bulk glasses achieved with near–IR excitation [49]

Through a continuous random skeleton being isotropic in 3–dimensions (3D), as seen in case of glassy Si, one cannot describe the ChGs structure. As_2S_3, As_2Se_3, GeS_2 and $GeSe_2$ could be regionally layer–like, on the other hand, pure S and Se are chain–like [45]. Raman (or inelastic) light scattering (RS) in a solid supplies structural and dynamic knowledge at a molecular level [46–47].

Near IR (NIR) Raman spectroscopy may be employed for analysing the materials being strongly absorbing in the visible range. In As–S–Se, the structure of ChGs, moving the excitation wavelength to 840 nm permits the achievement of high–quality Raman spectra with no material

alteration [48]. RC in the NIR could be initiated with the radiation of 840 nm from a tuneable Ti. The dominant property in 2–component sulphide and selenide compounds are the bands appearing at 345 ($As_{40}S_{60}$) and 230 cm^{-1} ($As_{40}Se_{60}$), regardingly [49] (Fig. 5). In Fig. 6 Raman spectra of a fresh, annealed, and photo–structurally altered As_2S_3 channel waveguide can be seen.

A strong broad band can be interpreted to the anti–symmetric As–(S, Se). In 3–component compounds with a S/Se=1 molecular ratio and declining as content, a rising decline in these broad band's intensity is noticed, being indicative of a decline in the number of As–containing pyramidal sites. New bands seen around 255 and 440–480 cm^{-1} appear in chalcogen–rich glasses and refer to Se–Se homopolar bonds. These units play a role as chalcogen chains connecting the remaining pyramidal units [50].

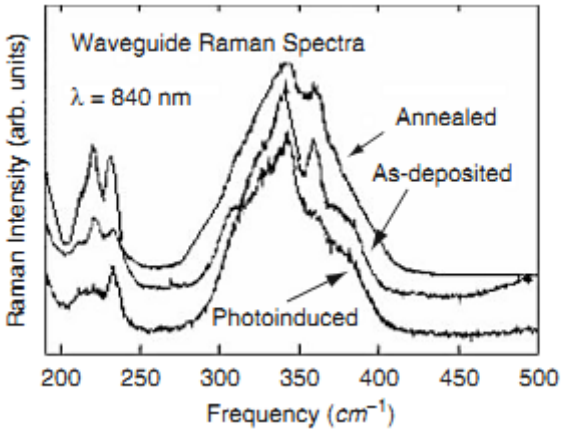

Figure 6. Raman spectra of a fresh, annealed, and photo–structurally altered As_2S_3 channel waveguide [49]

Moreover, these units are much more metastable and can be structurally modified or overcome with post–deposition process. Application of waveguide Raman spectroscopy (WRS) for the structural characterization of ChGs has been reported [51–52].

These sharp, molecular–signature properties have been pointed out not to be because of crystallinity within the film, but mostly due to the formation of as–deposited As_4S_4 units [50–53]. Rutherford back–scattering spectroscopy (RBS) yields quite useful information about the analysis of composition and structure of films, beside an accurate measurement of the film thickness [54].

Seal et al. employed x–ray photo–electron spectroscopy (XPS) to search for the composition of As_2S_3 at the film surface, comparing to that of the bulk glass and regarding diversity in the chemical bond's character and electronic structure. Ar^+–ion sputtering changes the glassy phase into a crystalline one. It has been also sorted out that, as films are lighted, some non–bridging S atoms have been detected but any non–bridging atoms seemed to appear in the case of the sample sputtered with an Ar^+ beam [55]. EXAFS works [56] inhibited the presence of chemical disorder in the structural skeleton of GaLaS thin films, although chemical ordering is dominant in GaLaS bulk glass. The structure of GLS bulk glasses has been searched for by Benazeth et al. [57] by employing EXAFS at the Ga K and La L_3 edges. The Ga and S environment in crystalline Ga_2S_3 is such that 2 of the 3 S atoms are linked to three Ga atoms and the 3rd S atom is linked to 2 Ga atoms. Lucazeau et al. [58–59] searched for these glasses' structure by Raman spectroscopy.

S and Se crystallize in numerous allotropic forms. The structures of S in solid, liquid and gaseous phases are complex, having many forms, such as S_2, S_3, S_6, S_7, S_8, S_9, S_{10}, S_{11}, S_{12}, S_{18}, S_{20} and S_∞.

The most thermodynamically stable crystal structure at ambient pressure and temperature is the insulating yellow orthorhombic α–cyclo octa sulphur (with 8–fold molecular rings, Fig. 7), which converts to a monoclinic β form above 94.5 °C.

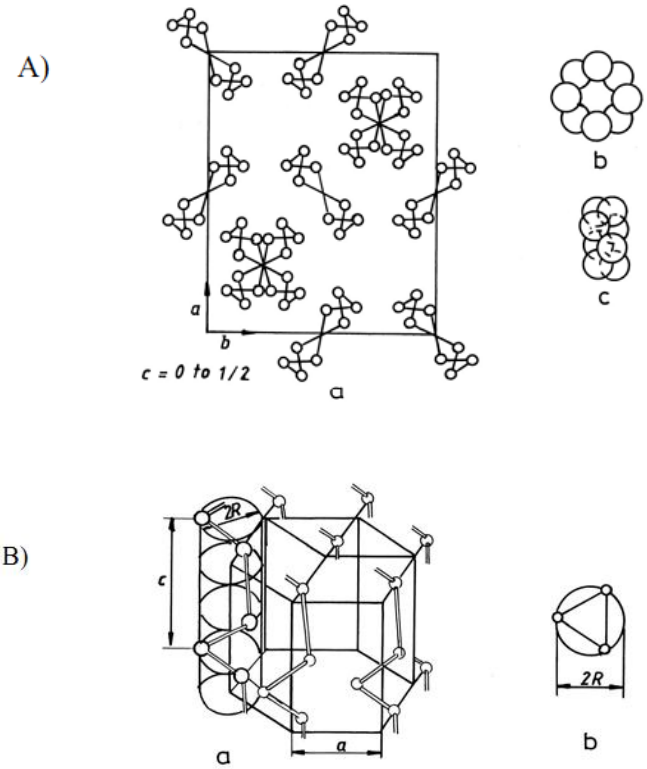

Figure 7. A) Unit cell of the orthorhombic α–cyclo octa sulphur (a); front (b) and side (c) view of the 8–fold molecular ring. B) Unit cell of hexagonal Se (a); chain view along the c–axis (b) [60]

Se also exists in different crystal structures, but most of them are metastable. The grey, hexagonal, photo–sensitive and semiconducting form of Se, consisting of helical chains of Se atoms along the c–axis, is the stable structure at all temperatures up to the melting point [61]. Te crystallizes in only one crystal structure, the hexagonal isostructural to Se, also being semiconductor, but with smaller gap than Se. The increase of metallicity along the group reflects the different structure types, going from insulating molecular crystals (O_2 and S_8–based) to cubic metallic Po, passing through semiconducting chained structures (Se and Te). Their thermal conductivity also reflects the increase of metallicity, being small for S (0.269 W m^{-1} K^{-1}, 300 K) and high for Po (20 W m^{-1} K^{-1}, 300 K). The reactivity of S, Se and Te, with metals decreases with the increase of the atomic number. S reacts at room temperature with alkali metals, Cu, Ag and Hg, forming sulphides, but it is necessary to melt Se and Te to make the metal selenides and tellurides. The three chalcogens burn in air: S and Se form two oxides, the dioxide and the trioxide, while Te, apart from these two, also forms the monoxide and the pentoxide.

Only one intermediate phase is reported in the S–Se binary system. It crystallizes in the monoclinic structure of γ–S [62–63] and is formed by a peritectic reaction at 85 at. % Se [64]. The existence of the crystalline compounds in the Te–S phase diagram is a controversial subject [4]. Se and Te form a continual solid solution between the two elements, which reflects their similar crystal structure and properties. It was determined that there were no 3 component compounds in the S–Se–Te system.

In the As–S and As–Se systems, three common compound compositions, As_2Ch_3, As_4Ch_3 and AsCh were reported, the first one being the most studied [60]. It has a monoclinic lattice (space group

$P_{21/c}$) that consists of extended layers of inter–connected 12 atom rings. The As–Te phase diagram has only a monoclinic As_2Te_3 binary phase stable at ambient pressure [65]. Concerning the S–Sb, S–Bi, Se–Sb, Se–Bi, Te–Sb and Te–Bi systems, only the common composition Pn_2Ch_3 (Pn=pnictide) exists, the number of phases rising with the increase of the chalcogen atomic number.

The structure of ChG depends on the system, preparation and history after the preparation. All of them can be described by four levels of structural characteristics [66]: (i) short–range order (SRO) of atomic arrangement (determined by the coordination number, bond lengths and bond angles); (ii) defect sub–system; (iii) morphology; (iv) medium–range order (MRO) of atomic arrangement (defined by network topology). This contrasts with the crystalline systems, where only the first two (single crystals) or three (polycrystals) levels are needed to describe their structures, reflecting the higher complexity of glasses.

S and Se form covalent bonds, forming molecules with the shape of rings or high polymer chains. Liquid S contains S_6, S_8 and other bigger molecules, up to very large macro–molecular rings and chains. Their relative concentration changes with temperature, being dominated by S_8 at low temperatures and by large chains and macromolecules at high temperatures. Vitreous Se also consists on Se_8 rings (~95 %) and chains (~5 %) of di–covalent atoms [67], while Te cannot be obtained in glassy state [60]. The dependence of the glassy chalcogen features on the preparation conditions and history is explained by the change of concentration of the species and degree of polymerization of molecules. Each S and Se atom in the glass has as nearest neighbours only two atoms from the same molecule, but the second coordination sphere has already contribution from atoms situated in neighbouring molecules [66].

Many binary ChGs were described based on the continuous random network concept. The predominance of covalent bonds can lead to SRO, due to local scale chemical order, and to the identification of structural motifs that act as basic building units. The way these units interlink gives the network topology, defining the MRO of the glass. Indeed, recent studies revealed the existence of MRO on ChGs, up to ~6 nm [67].

Most studies of arsenic ChGs have been made on As_2Ch_3 compositions. These materials were described with pyramidal $AsCh_{3/2}$ basic structural units. The tendency towards the glassy state is more evident in As_2S_3 than in As_2Se_3, being even weaker on As_2Te_3 [60]. Studies on glasses with other As/Ch ratios evidenced high concentrations of further environments, as Ch–Ch–Ch or Ch–Ch–As (Fig. 8) [68–69].

Si and Ge have a valence four on ChGs. The main structural units of $SiCh_2$ ($GeCh_2$) glasses are $SiCh_{4/2}$ ($GeCh_{4/2}$) tetrahedra, consisting on a central Si (Ge) atom bonded to four chalcogen atoms. Similarly, to the arsenic glassy materials, chalcogen enriched compositions present additional atomic environments, as chalcogen chains linking tetrahedra [66], while Ge enriched glasses also have $Ge(Ch_3Ge)_{1/2}$ structural units [70]. In ChGs the structural units are connected along edges or vertexes, which define their MRO [71].

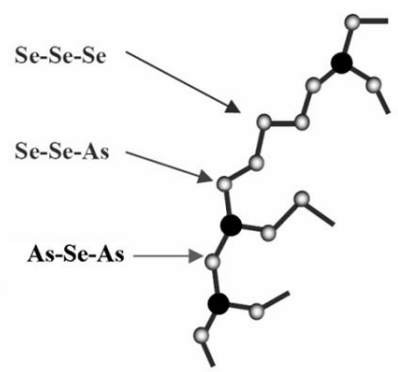

Figure 8. Model of As–Se glass, emphasizing the different types of atomic environments [69]

Glasses have three main types of short–range disorder: (i) distinct bond lengths, (ii) distinct bond angles and (iii) under–and over–coordinate sites [72]. In ChGs the different coordination number mostly results from dangling bonds (with an unpaired electron, C^o) and charged centres (or charged dangling bonds, C^+ and C^-) [73]. The disorder strongly affects the electronic structure, having in chalcogenide glasses more important role than impurities.

Because of the non–existence of long-range structural periodicity, all states of glasses have to be considered localized, as their Eigen functions could not be written using a periodic probability amplitude [74]. However, a discontinuity in the density of states can exist in the quasi–continuous states, similarly to the band gap of crystalline semiconductors. This discontinuity can have different origins, depending on the elements involved. In tetrahedrally bonded amorphous semiconductors (with Si or Ge) the sp^3 orbitals are split into bonding (σ) and anti–bonding (σ^*) states, which are the valence and conduction states, respectively. In the case of ChGs only 2 of 3 p states participate in the adherence, the remaining being a non–bonding electron pair (or lone–pair, LP). Therefore, albeit both the σ and LP states are occupied, the LP ones have higher energy and correspond to the valence states [75].

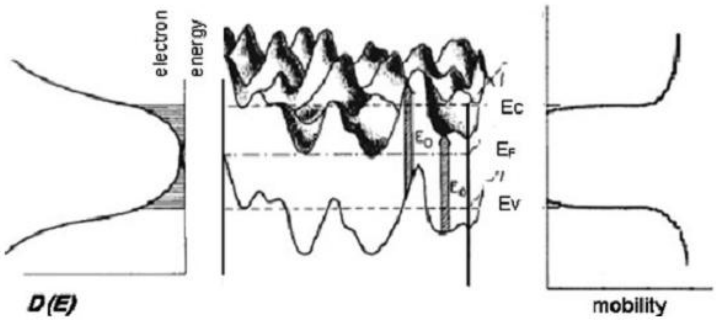

Figure 9. DOS (left), spatial fluctuations of mobility edges (centre) and the mobility (right) in semiconducting glasses, as a natural consequence of carrier energy [76]
Different bond lengths and bond angles led to tail regionalized states above and below σ and σ^*, where the carrier mobility declines to very low values, and mobility edges, defining a mobility gap, could be thought (Fig. 9).

In ChGs these tail states affect (extend) only the conduction states, the valence states being affected by tail states originated from interactions with LP. On the other hand, a large number of charged centres (10^{18}–10^{19} cm^{-3}) were proposed to exist [77], the positive and negative centres frequently approaching and forming valence alternation pairs (VAP's). The creation of these VAP's requires small energy in ChGs, which explains the large number of such defects [78]. The presence of a large number of VAP's on ChGs can be the reason why they are so insensitive to impurities, as a

change on the charge's ratio could compensate the existence of extra electrons coming from foreign atoms.

5. The Properties of ChGs

5.1. Thermal Properties

In ChG, the temperatures of glass transition (T_g), crystallisation and melting, besides the thermal expansion coefficient value (α), thermal diffusivity (TD) etc. are the thermal properties. T_g of ChG is regarding to the degree of adherent forces within the structural skeleton which has to be overcome for atomic movement [79–80]. Thermal conductivity (TC) of a material is caused by the energy transport through electrons or lattice vibrations (phonons). TC is related to phonon mean free path, that is T_g is noticeably narrower and correlatively TC is less. TD possesses a considerable role in switching showed by a ChG [81]. It determines the rate at which heat could be removed through the conducting channel. The presence of the strong correlation between TD and the switching manner of ChGs has been recently reported [82]. ChGs with low TD seem to inhibit storage manner and those of higher thermal diffusivity values can represent threshold–type switching.

5.2. Electronic band structure and Electrical Properties

When compared to impurities one can see that the electrical properties of ChG have considerably affected by the structural defects. The state's band appearing near the gap centre is due to specific defect characteristics of the material [83]. In order to elucidate or guess the features of a material in the band theory "Density of States (DOS)" diagram is employed [84].

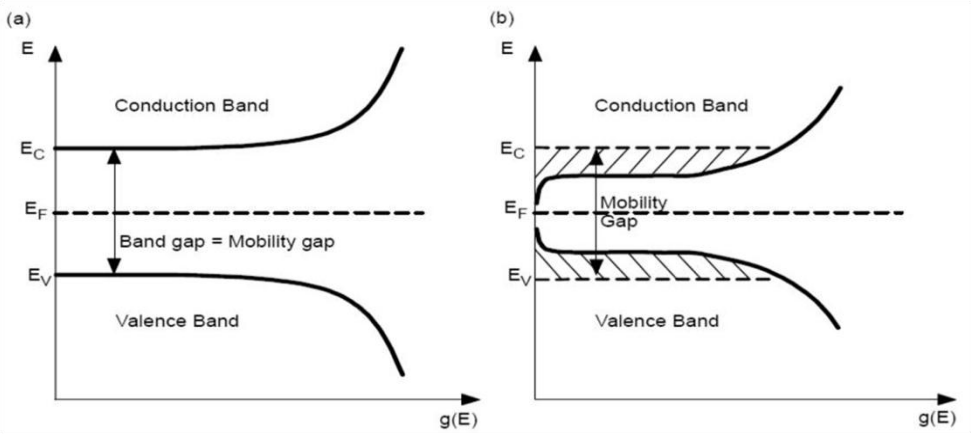

Figure 10. DOS models proposed by Mott (a) for a crystalline semiconductor, (b) for amorphous semiconductors [86]

Mott thought that the spatial wavings in the potential resulted from the configurational irregularity in glassy solids may cause the formation of regionalized states on the basis upon Anderson's localization principle [85]. He presented the DOS curve for crystal and the modification of it for glassy materials (Fig. 10) [86].

The first graphical presentation of the glassy semiconductor's band structure has been supplied by Cohen [87] referring as the Cohen–Fritzsche–Ovshinsky (CFO) model (Fig. 11). The related properties of the mentioned model can be given:

(1) Continual tailing of the regionalized states being very high that they overlap in the middle of the gap (Fig. 11–left hand side).

(2) The model guesses the presence of the moderate activity gap between the bands of valence and conduction.
(3) There is a finite density of these states g (E_F) at E_F. If g (E_F) > g (E_C), making solids to be metallic if not they could stay as semiconductors.

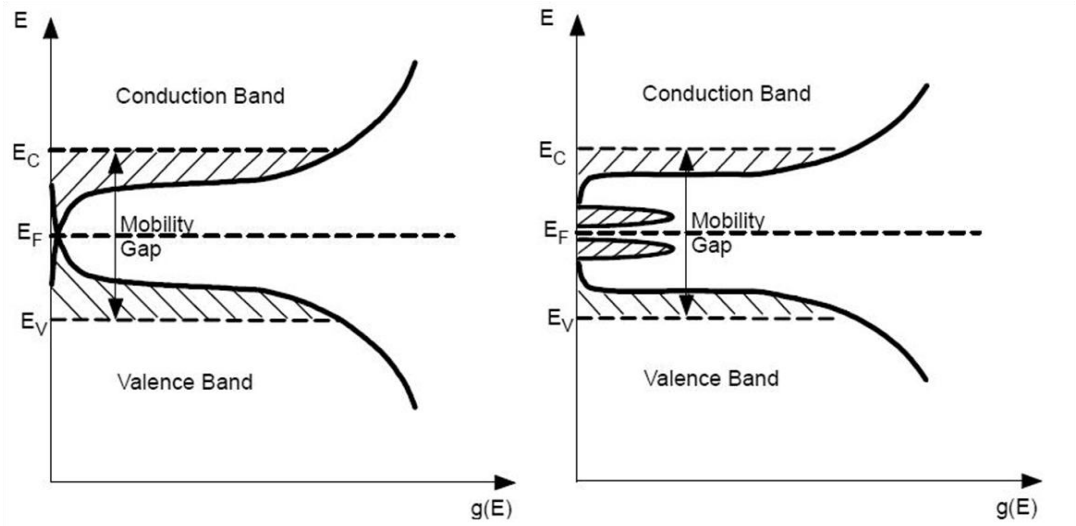

Figure 11. DOS models by CFO (left hand side) and by Marshall and Owen (right hand side). The striped zones designate localized states [88].

Emin also proposed another model named as small polaron model [89]. He has advised: the extra free carriers in some glassy semiconductor could enter as a self–trapped state due to the neighbouring atomic lattice.

5.3. Optical Properties

ChG's are potential candidates for photonic applications because of their noteworthy optical features, like high refractive index and photo–sensitivity and large optical non–linearity. The search made on the ChGs optical features is of noteworthy concern and supplies crucial knowledge of the relaxation mechanisms electronic band structure and optical transitions.

5.3.1. Absorption Spectroscopy

ChG's absorption curve is depicted in Fig. 12. In glassy semiconductors, the optical absorption edge spectra usually consist of 3 discrete zones:
A: High absorption zone ($\alpha=10^4$ cm^{-1}),
B: Spectral zone with $\alpha=10^2$–10^4 cm^{-1} is named as Urbach's exponential tail and
C: The zone $\alpha \leq 10^2$ cm^{-1}, being due to imperfections, covers low energy absorption and is caused by imperfections and impurities.

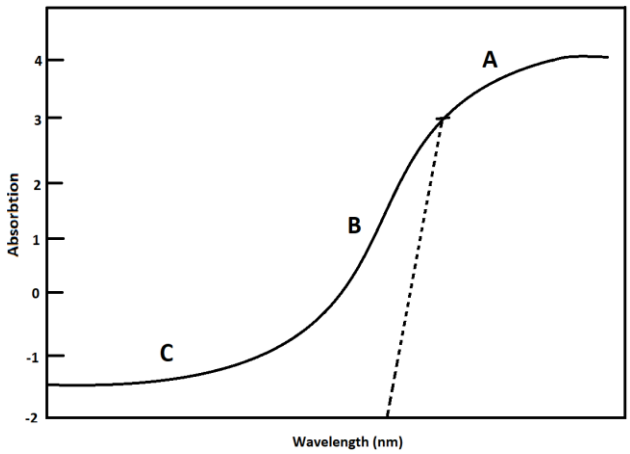

Figure 12. A typical absorption curve of ChG, indicating A, B, C regions [83]

5.3.2. Photo–induced Features

The photo–induced phenomena seen in ChG can be classified into 3 groups [83]:
The photon mode, in which the photo–electronic excitation directly incites atomic structural variations; the photo–thermal mode, in which photo–electronic excitation causes some structural variations thanks to thermal activation contribution; and heat mode, in which the temperature raise incited by optical absorption, is fundamental. Those phenomena seem to be in sulphides, selenides, and tellurides [83, 90].

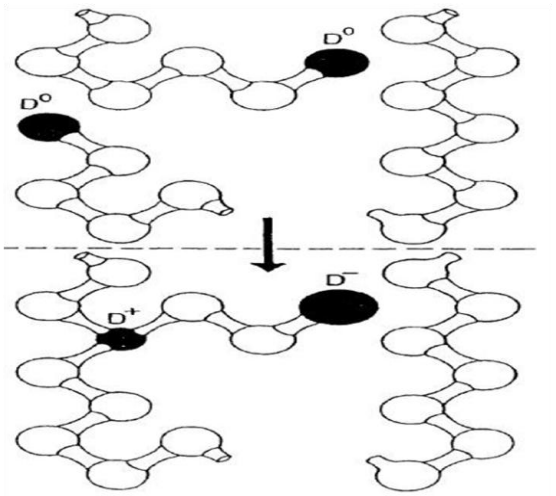

Figure 13. The occurrence of charged defects D^+ and D^- caused by 2 neutral defects DO [83]

The sensitivity of Ch–materials to the light and other electro–magnetic radiations is assumed as one of their interesting properties. Some of the important photo–induced (promoted) effects [83, 90–93] are **photo**–**darkening**, –bleaching, –expansion, –contraction, the effects of photo–plastic, opto–mechanical, a thermal photo–promoted transformation, photo–improved oxidation, photo–promoted softening and hardening, photo–elastic birefringence, switching (Ovshinsky), and photo–promoted fluidity and ductility, polarization dependent photo–plastic, photo–promoted dichroism, photo–promoted light scattering, **photo**–**luminescence** etc.

Photo–**darkening:** In ChGs the photo–darkening (PD) process is attributed to an optical absorption edge's movement to decline energies when the light whose energy is near that of the band gap is applied. ChGs seem to show the PD process to differing magnitudes [92–98]. Mott, Davis and

Street (MDS model) declared the first defect model [83], identifying the defects with negative correlation energy (Fig. 13).

The occurrence of a D^+, D^- pair from a broken Se–Se bond is governed by the exothermic reaction because of the strong lattice deformities which connote that the efficient é–é correlation energy is negative (negative U):

$$2D^0 \rightarrow D^+ + D^-$$

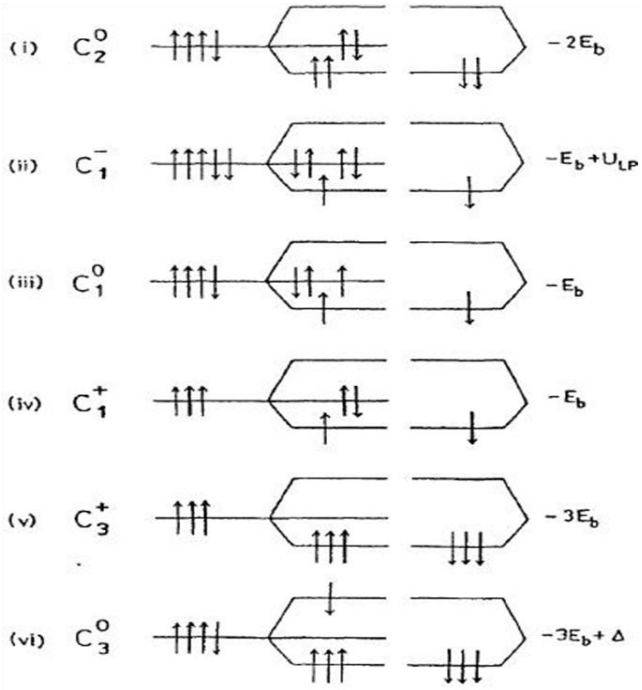

Figure 14. The Kastner, Adler and Fritzsche (KAF) defect's model in ChGs (Eь: the bond and, UL_0: the correlation energies). The arrows refer to the electron's spin state [90]

Fig. 14 illustrates various possible configurations of chalcogen atoms. Taking all the defects models of ChG and band models into an account Tanaka and Ohtsuka [92] presented distinguished PD model in which absorptional raise at constant wavelength is comparative to an intensity and factor supplying saturation at some maximum absorption. Liu and Taylor have further generalized the kinetic model for PD [92] (Fig. 15).

The straightforward process starts with an electronic excitation by a photon being absorbed at non photo–darkened site (Step 1 in Fig. 15). Those sites could be pre–existing imperfections or the sites could be an undistinguished atom or bond in an ideal glass. An atomic relaxation into a new local atomic configuration (Step 2), electronic relaxation (Step 3), and further relaxation into a metastable configurational defect (Step 4) follow the excitation.

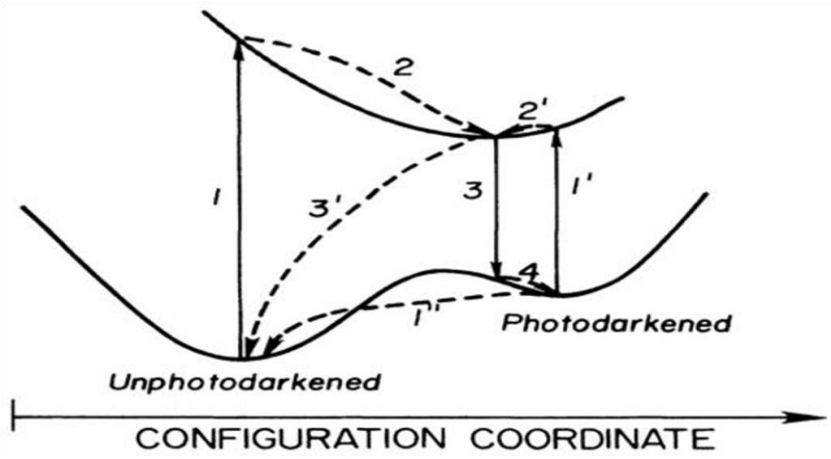

Figure 15. Configurational diagram indicating the formation of metastable defects [92]

Photo–luminescence (PL): The impairment states in the band– openness of ChG are supposed to possess a valuable role in the formation of most of the photo–improved phenomena, as impairments are thought to modify their charge conditions or mutual engagement by trapping photo–induced carriers. In order to examine those gap–states, photo–luminescence measurement is an efficient means as their spectra supply further knowledge about the relaxation process of photo–induced electron–hole pairs [99]. Photo–luminescence spectra in bulk ChG have been initially seen [83, 100]. Seki and his colleagues [101] recently reported that the conduction band model for the origin of photo–luminescence in Ge–S glass by the recombination of é regionalized at the bottom of conduction band and holes captured by the charged imperfections. Aoki et al. elucidated the inspection of double–peak life time distributions in g–As_2S_3 and a–Se Chs by self–trapping excitation model [102]. Luminescence in semiconductors takes place because of the é–hole recombination and its basis could be trailed to 6 different transitions (Fig. 16) [99]. The configurational coordinate diagram assumed to be an appropriate way to show luminescence processes in ChG is given in Fig. 17.

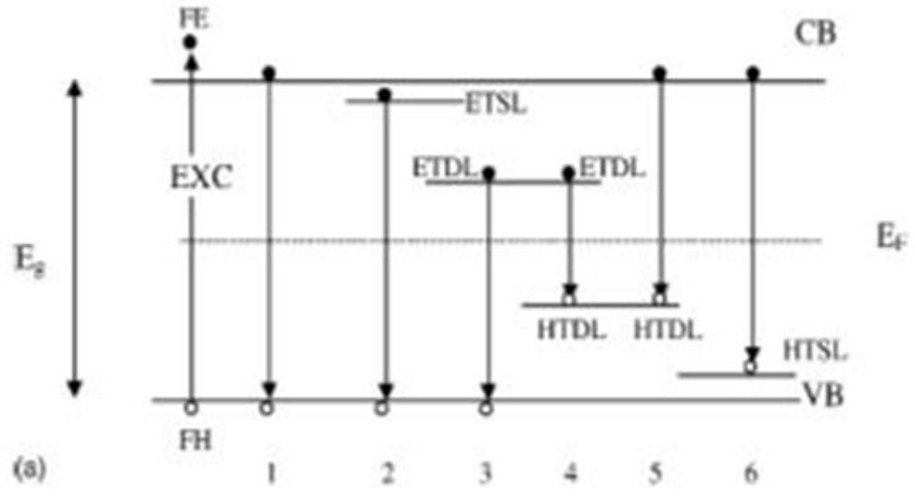

Figure 16. Schematic presentation of the transition involved in ChGs (FE: free é, FH: free hole, ETSL/HTSL: é/hole captured in a shallow level, EDTL/HDTL: é/hole captured in a deep level and, ETDL and HTDL: é–hole pairs captured in impairment pairs deep in the gap) [103]

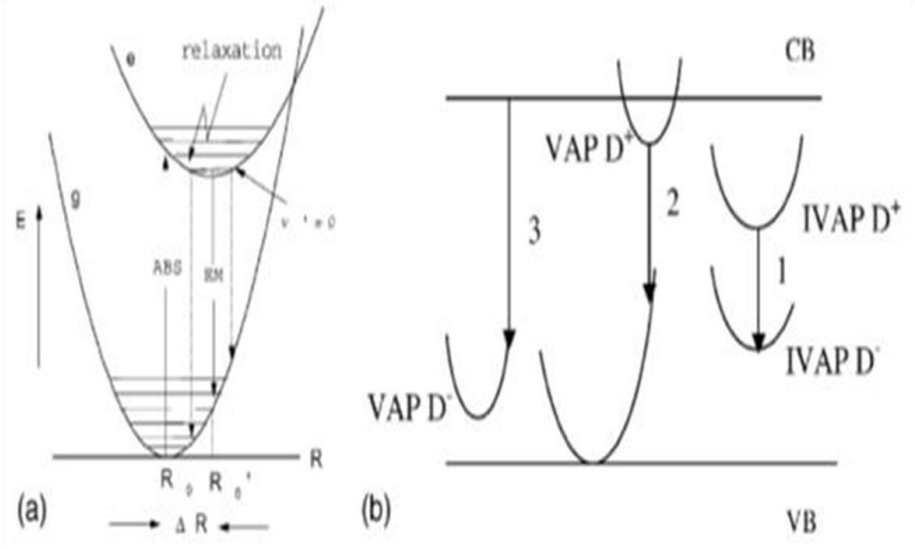

Figure 17. Configurational coordinate diagram presenting (a) the absorption and emission transitions, (b) the multiple transitions in a ChG semiconductor (VAPs: valence modification pairs and IVAPs: inverse valence modification pairs contributing to luminescence in ChGs) [103]

5.3.3. Optical Non–linearity

2–photon absorption spectroscopy, 4 wave mixing, Z–scan, 3rd harmonic generation and optical Kerr shutter were employed to determine non–linear refractive index besides Ch solid's non–linear absorption coefficient [104–105]. 2–photon absorption (β) and intensity–dependent refractive index (n_2) on linear absorption and refractive index for an ideal glassy semiconductor are given in Fig. 18.

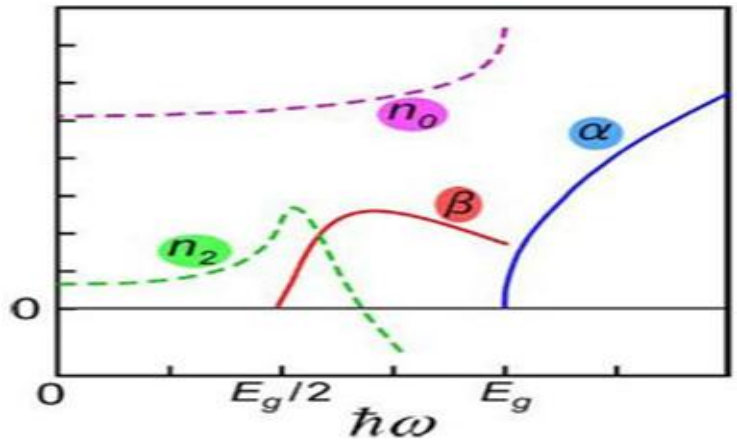

Figure 18. Spectral dependence of α, n_0, β, and n_2 in an ideal glassy semiconductor with energy gap E_g [104].

Sanghera and his co–workers [105] made a comparison on the non–linear optical properties of these ChGs in the forms of both bulk and fibre. In the applications based upon telecommunications, ChGs became standout because of exhibiting 3rd–order optical non–linarites (Kerr, Raman and Brillouin) between 2 to 3 orders of degree bigger than SiO_2.

The non–linear absorptions generally inhibited in glassy semiconductors are depicted in Fig. 19.

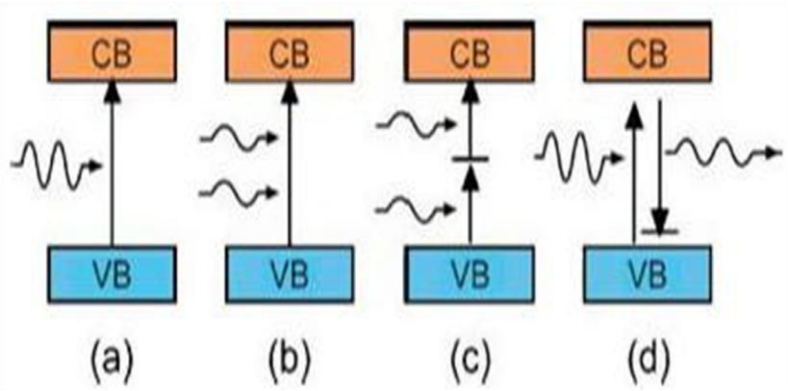

Figure 19. Schematic presentations of (a) 1–β, (b) 2–β, (c) 2–step absorption through a midgap state, and (d) RS process in a semiconductor with a valence (VB) and a conduction band (CB) [104]

The possibility of a solid absorbing more than 1 photon, before it relaxes to the ground state, could be considerably improved at sufficiently high intensities [104–105]. According to many reports it is indicating that a 2–β process is liable for optical non–linarites inspected in ChGs [106–108].

6. Glass Formation and Production of ChGs

The glass formation tendency of Ch system is defined by the chemical bond's character between the atoms that form the glass. Glass formation is easier in systems containing atoms that will bind by predominantly covalent chemical bonds. As stated in Fig. 20, large vitreous domains exist in the Ge–As–S and Ge–As–Se systems. A much narrower vitreous domain exists in the corresponding Te system. This can be explained by the increased chemical bond's metallic character in tellurides and therefore their increased delocalisation in space, more favourable to redistribution of atoms at high temperature [109–110].

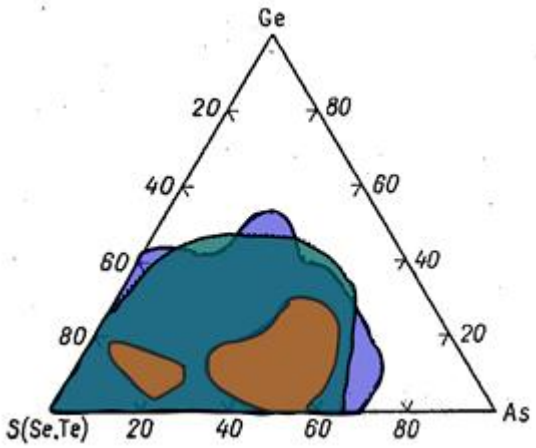

Figure 20. The glass formation regions in the Ge–As–S (blue), Ge–As–Se (purple) and Ge–As–Te (brown) systems [109]

A very important criterion to predict the ability of a given composition to give a glass is the critical cooling rate (CCR) of the corresponding melt [110]. It gives the cooling rate that must at least be achieved to avoid the crystallisation process to take over during solidification. The higher (lower) the critical cooling rate, the more (less) probable is the crystallisation at the melt solidification. Table 1 gives the CCR for some binary and ternary ChGs [111]. As_2S_3 and $As_2S_{1.5}Se_{1.5}$ have very low CCR. Even when slowly heated, As_2S_3 does not crystallise before melting. On the other hand, As_2Se_3 and $As_2Se_{1.5}Te_{1.5}$, that exhibit CCR higher by three orders of magnitude, can be crystallised

during heating. Ge–S and Ge–Se system's glasses possess a stronger tendency to crystallise than of the As–S and As–Se system's glasses [112].

Table 1. Thermal characteristics and CCR of some ChGs [111]

Glass	Tg (°C)	T_c (°C)	T_l (°C)	T_c-T_g (°C)	CCR (K/s)
As_2S_3	185	-	310	-	2.4×10^{-6}
As_2Se_3	170	298	370	128	9×10^{-3}
GeS_2	495	550	820	55	17
$GeSe_2$	380	580	740	200	1
$As_2S_{1.5}$ $Se_{1.5}$	175	-	-	-	-
$As_2Se_{1.5}$ $Te_{1.5}$	150	231	300	81	5×10^{-3}

CCR change with compositions in a given system. 50–100 g of a melt of $GeS_{2.06}$ composition with a CCR of 3 K/s can be transformed into a vitreous state by cooling in air while 2 g of $GeS_{1.94}$ melt with a CCR of 40 K/s already need a more efficient quenching process such as water quenching to give a glass.

The vitreous domain for a given system strongly depends on the glass elaboration process. For example, quenching from the melt in air allows obtaining Ge_xTe_{1-x} glasses only in the close vicinity of the eutectic composition, $Ge_{15}Te_{85}$, while amorphous thick films of several microns in thickness with $10<x<45$ are obtained by thermal co–evaporation [113].

The most common way to prepare a ChG is the solidification of the glass–forming melt. Unlike the oxides, the preparation requires an oxygen–free atmosphere. For this reason, the synthesis is carried out in an evacuated sealed quartz ampoule. The initial charge of ChG, usually comprising the constituting elements weighed in stoichiometric quantities, is placed in the ampoule, melted and further quenched. The synthesis conditions (time, temperatures) are highly dependent on the glass nature. For example, the presence of an element with a high vapour pressure such as S requires a slow heating to avoid building too much pressure in the tube. The quenching conditions (air quenching, water quenching, ice water quenching) need to be adjusted according to the intrinsic property of the glass, its critical cooling rate in particular, but also the charge mass, as indicated above for Ge–S glasses.

The preparation of high purity glasses is required for optical applications. In this case, the commercial elements (As, Ge, S, Se or Te), which usually contain 1–100 ppm wt. of hydrogen, O and C, need to be purified previous to their use in synthesis. Moreover, oxidation of Se, As or Te is difficult to avoid since it occurs in normal conditions, even at room temperature. A way to get rid of As and Se oxides is to take advantage of the higher vapour pressure of the oxides compared to the elements and proceed to their selective evaporation. Such a technique cannot be used with Te. The dissolution of the Te oxide impurities in hydro bromic acid is then the way to purify the element. A further purification of the glass forming Chs can be achieved by a chemical distillation: the batch is introduced in the hot part of a double chamber vessel and the distillate is recovered in the cold chamber. Getters can be used to get rid of some impurities. For instance, for binding the oxygen–containing impurities, it is possible to use micro amounts of aluminium or magnesium, leading to low–volatile Al_2O_3 or MgO during melting, while for binding the hydrogen–containing ones it is possible to employ chlorine and chlorides of glass–forming elements, leading to hydrogen bound to HCl. The glass charge is then melted at about 700 °C and further subjected to distillation.

When these steps of purification are completed, heat treatment and further quenching of the purified batch need to be carried out. At these points, other types of impurities need to be tracked. For

example, reaction can occur between the silica tube and the reactants. Choice of synthesis temperature is crucial. It has been shown that $Ge_{25}Sb_{10}S_{65}$ glass samples contained microscopic inclusions of 5–50 μm in size in concentration of 10^4–10^6 cm^{-3} when prepared at 800 °C and inclusions of 80–500 nm in size in concentration 10^8–10^9 cm^{-3} when prepared at 950 °C [114].

While the preparation in evacuated sealed ampoules is the most common way of preparation of ChGs, other ways exist, for example, when the usual quenching in air or water is not enough to avoid crystallisation: from the simple crush of a droplet between two plates to more sophisticated techniques, such as twin roller quenching operating in an Ar–filled glove box. In this technique, droplets of melt are laminated in between two rotating Cu rollers to give flakes of thickness ~0.1 mm. It allows obtaining quenching rates of about 10^6 K/s. This method has mainly been used for the elaboration of Li^+–conducting chalcogenide glasses [115].

Mechanical alloying or high energy milling was also proposed to produce ChGs. A jar containing both the precursors of the glass and hard balls is placed in a planetary ball mill apparatus. Rotation cycles of selected time and speed allow producing a solid-state reaction between the precursors at low temperature, much below the melting temperature. Li^+–conducting glasses of the system Li_2S–P_2S_5 were prepared in this way [116] but also the Ge–Ga–Se system optical glasses [117]. In the last case, the powders were further sintered by spark plasma sintering leading to the production of large pieces of bulk glasses.

Many physical and chemical ways of deposition have been proposed to produce chalcogenide thin films [118] thermal evaporation under vacuum (classical, flash, co–evaporation, e–beam evaporation) or various sputtering techniques (RF sputtering, reactive sputtering, magnetron sputtering). Classical thermal evaporation is used for the deposition of amorphous Se for flat–panel x–ray detectors for example [119]. For binary or ternary compositions, such as Ge–Te, when preferential evaporation can occur, thermal flash evaporation or thermal co–evaporation can be preferred [113, 120]. Deposition of complex Ch compositions is usually carried out by sputtering techniques with the preparation of multi–component targets. A popular example is the preparation of phase–change materials Ge–Sb–Te or Ag–In–Sb–Se films for the development of optical memory [121]. Pulsed laser deposition has been used to deposit very complex compositions, such as rare–earth doped Ch amorphous films for optical applications (e.g. Ge–Ga–Sb–S: Dy_2S_3) [122] and ion–selective thin film membranes for the detection of heavy metal in solution [e.g. Pb(Cd)–Ag–As–I–S] [123]. Chemical vapour deposition based upon the use of gaseous precursors (e.g. GeC_{14} and H_2S for Ge–S films) was proposed [124]. Spin coating of Ch thin films, e.g. As–S films, is achieved by taking advantage of the ability of Ch to dissolve in amine solvents [125].

7. Application Fields of ChGs

Since early 1970's there have been many researches on ChGs as promising integrated optics materials [83, 101]. The IR transparency of ChGs results in a large variety of optical applications as presented in Fig. 21. ChGs possess the capacity to be the principal for future optical computers, much as Si is the principal for today's micro–processors and computer storages [105]. Any optical micro–circuit is expected to request passive instruments like waveguides and gratings to control the flow of optical information between the active elements, which could be produced in a ChG by means of various methods covering photo–darkening and photo–doping [106]. Grating could be noted on Ch bulk and thin films. The photo–sensitive answer of ChGs could be employed to achieve high–resolution appearances and photo–lithographic resists [126]. High–speed optical switching were presented with ChGs [127]. ChG fibres find themselves application in the several fields thanks to their high band–gap, long–wavelength multi–phonon edge and low optical attenuation [128]. They are also chemically steady in air and could be drawn into long core–clad

fibres, and possess the potential to allow new applications being unattainable with current IR materials [128–131] (Fig. 21).

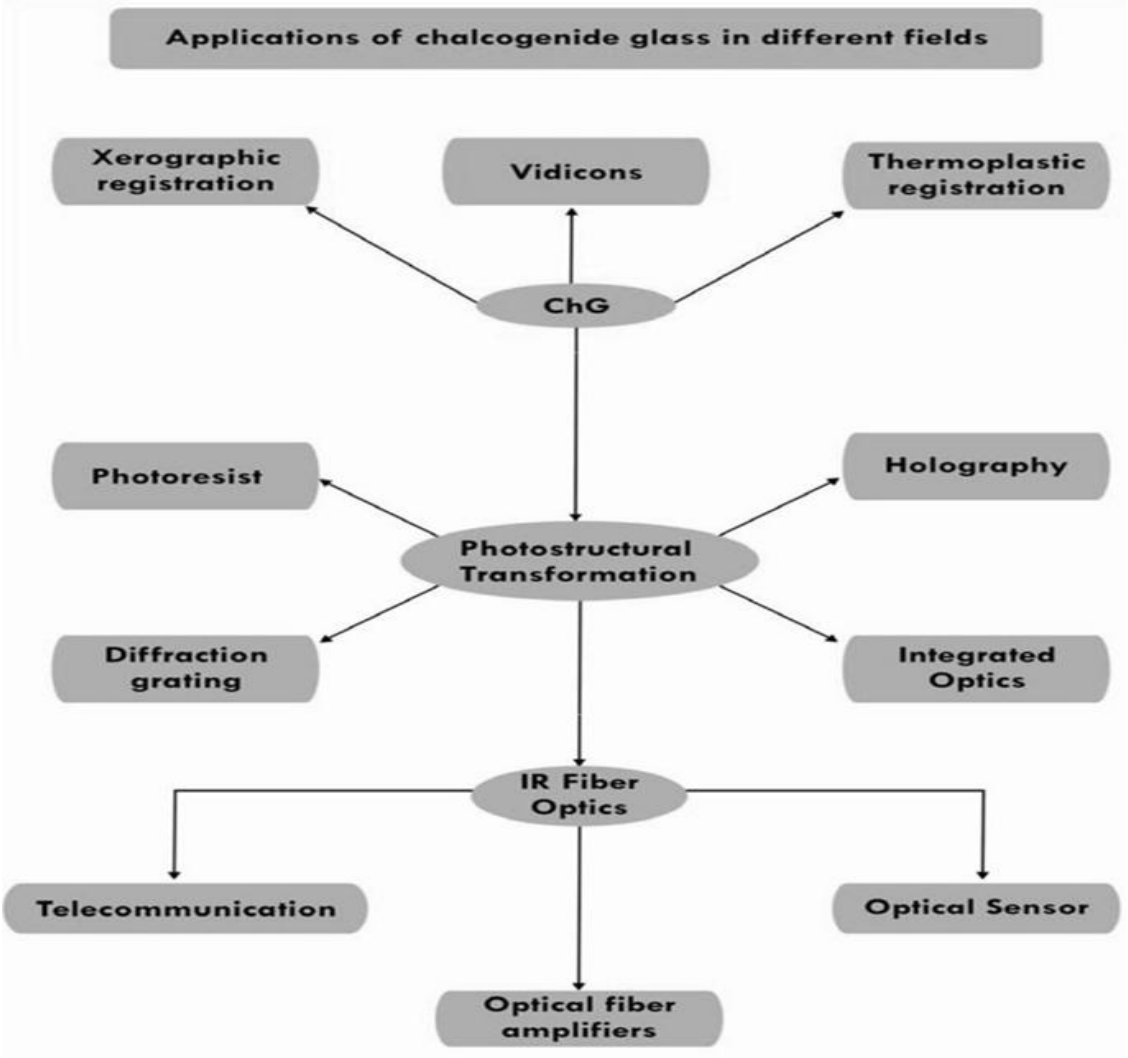

Figure 21. Applications of ChG in different fields [132]

7.1. Infra–red Optics

The most noteworthy property of ChGs is associated with their transparency in the mid and far IR depending on the glass composition (S, Se or Te–based composition). ChGs were quite recently of surpassing attraction for night–vision instruments thanks to their notable transparencies in the 2 atmospheric windows (3–5 and 8–12 μm) (Fig. 22 a). Since everyone and every sort of object, near room temperature (RT), possesses its maximum radiation in 8–12 μm IR range, this characteristic is at the basis of many practices, like IR optical lenses. Indeed, ChGs tend to replace, at least partially, the expensive mono–crystalline Ge or ZnSe (Figs. 22 b–c). Easy processing and the lower cost of ChGs comparing to mono–crystalline Ge or ZnSe led them to be one of the best candidates for mouldable lenses. For example, the Ch lenses GASIR® (Ge–As–Se) is nowadays commercialized by Umicore (Fig. 22 d). Thermal cameras (TC) are originated upon the reality that everyone and every sort of object, near RT, radiates in the IR range. Such a radiation is more noteworthy when body heat or given object raises (Fig. 22 e).

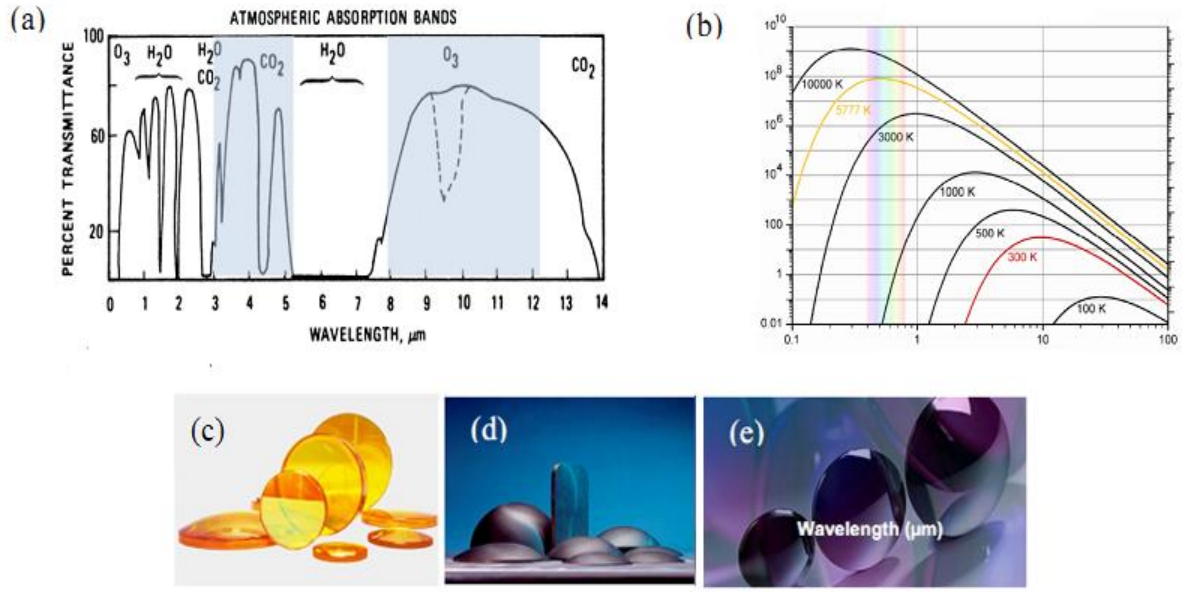

Figure 22. (a) Atmospheric transmission, (b) Spectral radiability of an excellent blackbody at differing temperatures, (c) ZnSe lenses, (d) Single crystal Ge lenses, (e) GASIR$^{(R)}$ glass lenses

As well as military applications, thermal cameras are very suitable in many civilian application's field. They can be employed by mechanics or electricians to sort out over–heated assemblies in electric fittings or power transfer lines. Firemen could also evaluate them to observe if there is anybody in a house on fire and to rescue them (Fig. 23 a). The medical imagery is another noteworthy application. In such case, a TC is employed as a body thermometer to sense local heat raise, that can be the signs of a vascular problem, infection or tumour. Finally, one of the most recent applications is systems for driving support, like those in new generation BMW cars (Fig. 23 b).

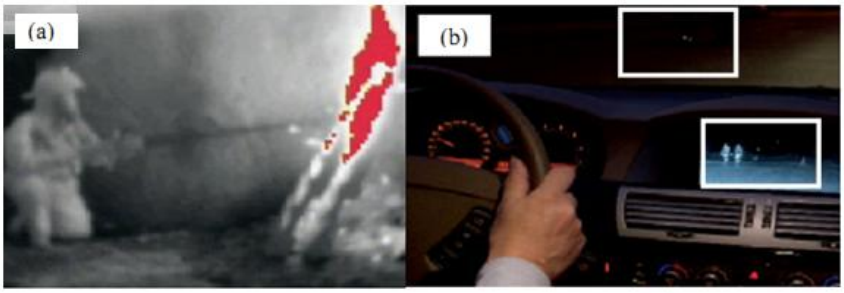

Figure 23. Examples of civilian applications of thermal cameras (a) house on fire, (b) driving assistance [133]

7.2. Optical Sensors

Because all living cells and chemical compounds (solid, liquid, gas) usually possess fingerprint absorptions in IR range, ChGs are gripping materials for medical applications, chemical analysis and are very promising and of high concern in spatial applications, such as to designate gas signs on exo–planets [134–135] (Fig. 24 a). These waveguides are employed as optical sensors to employ fibre evanescent wave spectroscopy to search for, at molecular level, various troubles faced with in microbiology, such as the differentiation between sane and tumoral cells, in the protection of environment to display pollutant in waste water [133] or in food security. The IR beam enters the waveguide, the light is reflected several times inside the waveguide and these internal total reflections lead to the formation of a deciduous region at the waveguide's surface, penetrating in the air on few μm. As the surrounding medium (substance to analyse) absorbs, the deciduous zone is absorbed at each reflection. Afterwards, the characteristic absorptions of the substance to be

analysed (Figs. 24 b–c) affect the light collected at the output. Fig. 24 d shows the IR signature of different bacteria encountered in food safety control [136].

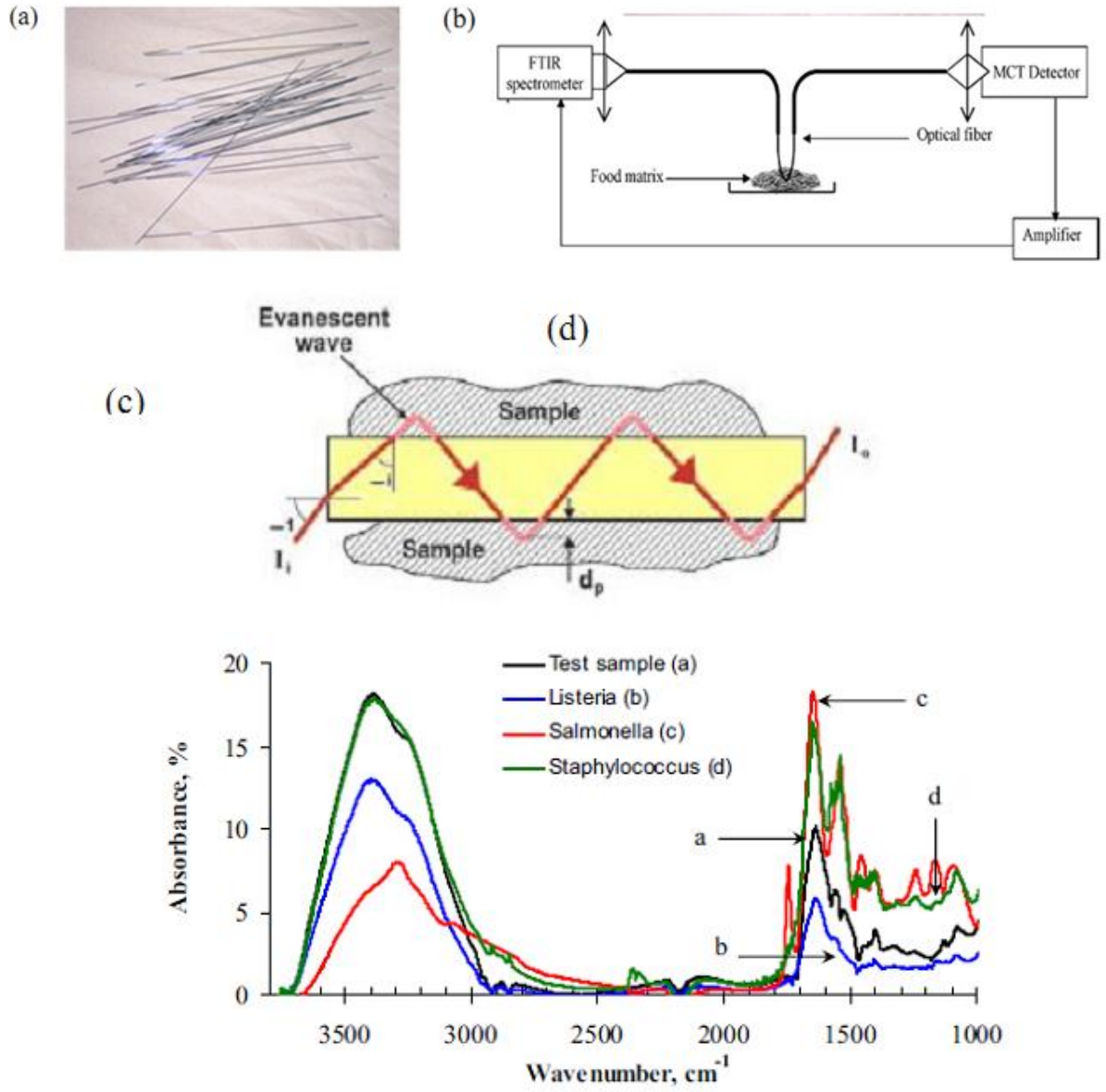

Figure 24. (a) Photographs of chalcogenide fibres of 400 μm diameter, (b) Scheme of the IR light propagation in the waveguide (fibre) and indicating the evanescent wave penetrating into the sample on few micrometres, (c) Set–up to measure the IR signature of one given sample, (d) IR signature of different bacteria [136]

7.3 Electrolyte for Solid–state Batteries

Li–ion battery is an assembly of three materials: anode, electrolyte and cathode. Anode and cathode are mixed electronic/ionic conductors, while the electrolyte is a pure ionic conductor. Common Li–ion batteries based on liquid electrolytes (Fig. 25 a) have conquered the electronics marketplace; however, cost and safety are the over–riding parameters limiting their widespread use in electric vehicles or hybrid electric vehicles. All solid–state batteries offer good safety (no leakage of liquid electrolyte, no risk of explosion) and easy fabrication (Fig. 25 b).

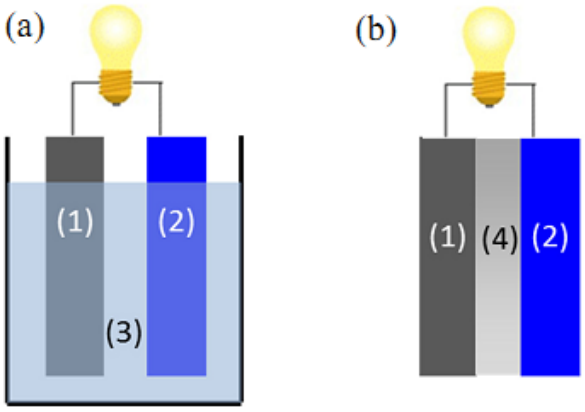

Figure 25. Scheme of a battery with electrolytic solution (a) and solid electrolyte (b) (1: anode, 2: cathode, 3: liquid electrolyte, 4: solid electrolyte) [137]

ChGs are among the Li^+ ionic conductors with highest electrical conductivity, which make them very promising as electrolyte for solid–state batteries as shown by Tatsumisago [137]. The glass composition $70Li_2S–30P_2S_5$ exhibits upon heating the formation of $Li_7P_3S_{11}$ crystals, leading to the very high ionic conductivities of about 10^{-3} $S.cm^{-1}$ at 25 °C [138], which represents an increase of about two orders of degree when compared with the base glass.

8. Recent Trends in ChGs

Instrument applications employing ChG generally request the glass to be processed into the forms of fibre or thin film. Traditionally, Ch–films are collected by physical vapour deposition (PVD) methods like thermal vaporization, pulsed laser deposition or sputtering from the bulk melt quenched ChG [139–143]. In general, when the laser deposition and sputtering matter they are largely restricted to 2–D surfaces and need high–vacuum processing and sometimes difficult target preparation. Another restriction, especially for thermal vaporization, is that the film resulted often possess a varying stoichiometry, because of variational volatilization in multi–component materials. Solution–based coating methods are used to solve this problem [144].

8.1. ChG as Nano–material

Nano–colloids of ChG recently attracted lots of interest in the research fields [145–149]. Apprehending the glass chemical endurance and discovering the appropriate solvent for preparing solutions is quite critical when preparing nano–colloids. Laser wearing method has been used for preparing aqueous As_2S_3 colloidal solution by Ganeeva et al. [150].

Berzelius and Bineau used another preparation method of Ch nano–colloid, re–organising the dissolution of As_2S_3 in liquid ammonia [151]. Afterwards, numerous numbers of structural and optical searches have been conducted on Ch nano–colloid produced by dissolving in various kinds of solvents as ethylene diamine, n–butyl amine, n–propyl amine, diethyl amine, tri methyl amine and other organic solvents [152–164]. Chern and Lauks [158–160] supplied important aid in the field of nano–colloid ChG such as As_2S_2, As_2Se_3, As_2Te_3 and Ge–Se. The dissolution product of As_2S_3 and $Ge_{23}Sb_7S_{70}$ in amine solvent is stated in Fig. 26 [161].

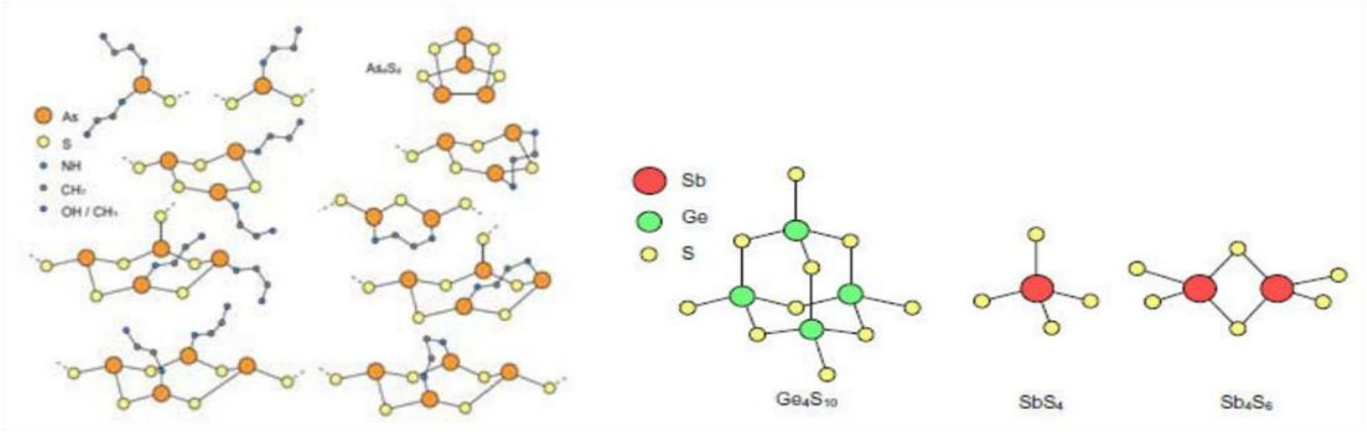

Figure 26. Structure of dissolution product of (a) As_2S_3, (b) $Ge_{23}Sb_7S_{70}$ in amine solvent [162]

Thin films produced from nano–colloid $Ge_{23}Sb_7S_{70}$ ChG were declared to be of promising optical features. In 2010, Ch opal and inverse opal photonic crystals have recently been achieved from nano–colloid $As_{30}S_{70}$ ChG by Kohoutek and his colleagues [163]. The produced photonic structures from nano–colloid $As_{30}S_{70}$ and SiO_2 as supplied in Fig. 27, are prescribed for designing novel flexible colloidal crystal laser instruments, photonic waveguides and chemical sensors.

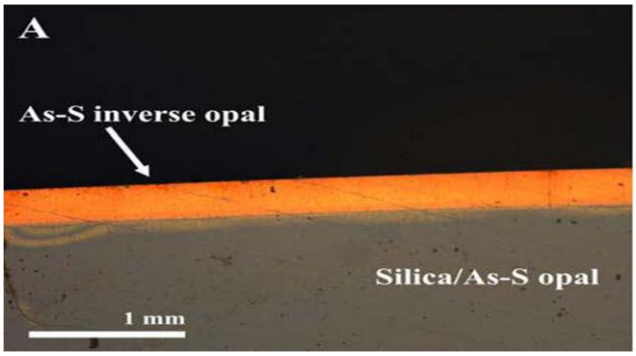

Figure 27. Photonic structures of nano–colloid $As_{30}S_{70}$ and SiO_2 [163]

The solution originated synthesis of photonic structures based upon ChG have extensive application in various optoelectronics' areas.

8.2. Chalcogenide/polymer Nano–composite Films

Great concern presently dedicated to the production of new generation materials appropriate for photonics applications. Among these, the glassy Ch structures are of noteworthy concern because of their effectiveness in non–linear optical characteristics [164–173].

Kohoutek [167] recently produced Ge–Se/poly styrene (PS) dielectric and Au/Ge–Se /PS/dielectric reflectors produced from glassy Ch and polymer films with the optical reflectivity (R) greater than R > 99 % near λ ~1550 nm by low–temperature and low–cost deposition methods. Thin polymer films anchored to ChG are largely employed for modulation of the surface features and the preparation of versatile adaptive surfaces being capable of meeting environmental changes.

8.3. ChG Fibers

Optical fibres require low–phonon–energy materials exhibiting marvellous endurance to humidity corrosion and good glass forming capability. The only glassy materials accomplishing those needs are S, Se, or Te glasses [174]. Ch–fibres and ChG fibres incorporated with rare earths were examined for active applications in near–and mid–IR [175–181]. Arsenic trisulphide glasses possess weak rare–earth solubility and depict crystallization signs occurring at the same time with the fibre–drawing temperature. Ge–As–Ga–Sb–S glass incorporated with Nd–Ch fibres inhibited an optical amplification at 1.083 μm with a maximum internal gain of 6.8 dB received for a pump power of 180 mW [180]. ChG fibres find themselves an application in all optical switches and fibre lasers [181]. Holey fibres based on Ga–La–S glasses ChGs are recently introduced [182]. Reviewing on the Ch–holey fibres by Trolès and his co–workers [183] says holey fibres possess the potential for new applications in the area of high non–linear optics and large mode–area propagation together with single–mode operation at all wavelengths.

8.4. Nano–composite ChG Fibre

The optical features of quantum dots gained into poli methyl metacrilate fibres produced by physical methods have been pointed out [137]. Nano–scale enforcements attracted widespread interests in the polymer field, because reinforced materials (composites) supply better structural mechanical properties when compared to the pure polymers. Semiconducting nano–particles (quantum dots) were those of interest when it comes to polymer reinforcement because of their exciting properties, especially their excellent size–dependent optical ones [138].

8.5. Micro–structured Fibres

The conventional way of routing light into an optical fiber is to employ 2–index configuration. The guide's core is made of a glass possessing a refractive index which is slightly superior to its coating. In such a way, IR light generated by the reflection in the core/coated interface stays in the core of the fiber and is emitted [184].

An original way to achieve single–mode fibers is to design micro–structured optical fibers (MOFs), which supply unique optical features because of high degree of freedom to design the geometric network. Since it primarily searches upon silica MOFs [185], this new generation fiber class indicated great attraction in the optical fiber society. In such a situation, the light emission is achieved in high refractive index core enclosed by a few crowns of low refractive index air vents. After 10 years, MOFs were performed with ChGs [186].

Low optical losses and new generation Ch MOFs, like small core fibres, exhibit strong attraction for wavelength conversion by employing non–linear effects like 4–wave mixing, Raman and Brillouin scattering and super continum generation [187]. Those original sorts of fibres are very appropriate to see evanescent spectroscopy in filling the hole by a gas to be analysed. They could be employed for effective mid–IR sensing [188].

8.6. Ch Micro–structured Optical Fibres for Mid–IR Applications

The casting method is well adapted for the realisation of Ch micro–structured optical fibres. Trough the mentioned process, high–quality non–linear fibres were prepared with optical losses smaller than 1 dB/m. Strong non–linear effects were observed in such fibres and allowed to notice high–speed wavelength conversion and generation of super continuum in the mid–IR. Moreover, Ch fibre's IR transmission allows the conception of IR sensors. The high delicacy of a micro–structured fibre with an exposed core was depicted through evanescent wave spectroscopy.

Additionally, a single–mode polarization–keeping MOF covering the mid–IR region from 3 to 8.5 μm was achieved [189].

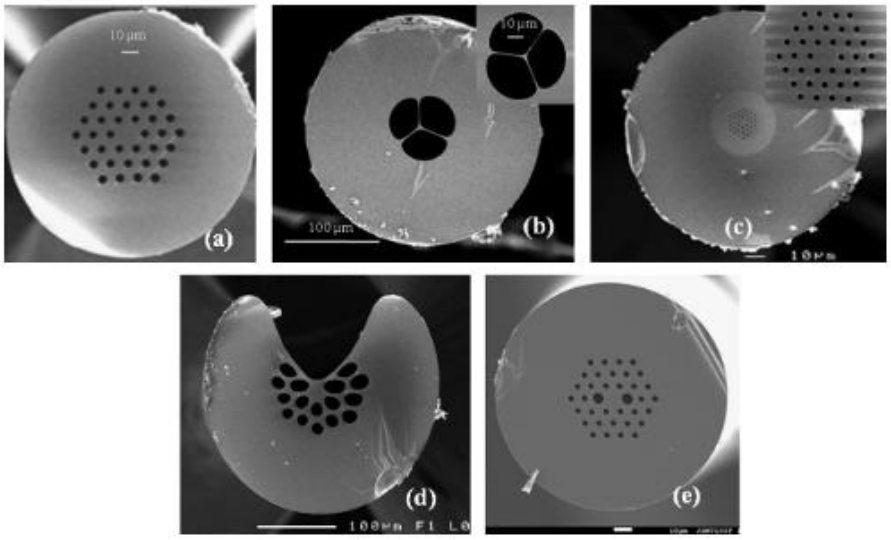

Figure 28. Various geometries achieved with ChGs: (a) 3–circle expansive–core fibre, (b) small suspended core [190], (c) 3–circle small–core fibre [191], (d) exposed core fibre [188], and (e) highly birefringent fibre [192]

9. Conclusions

ChGs have a high interest in several fields of applications, actually being the subject of researches in many academic and non–academic teams worldwide. Their large transparency in the IR range, tuneable electronic structures (depending on the chalcogen element), low thermal conductivity and high polarizability, despite of their drastic synthesis conditions, make these glasses very attractive. They can be shaped as optical lenses, drawn into fibre or can be sputtered as thin films to be used as optical sensors or phase change memories. The main drawback of ChGs remains their poor mechanical properties. However, the controlled crystallization of the base glass thanks to a thermal treatment that leads to glass–ceramics materials can overcome this limitation. Depending on the crystal composition, the electrical (electronic/ionic) properties can be also considerably enhanced, as demonstrated in the Li_2S–P_2S_5 system.

References

[1]. Elliott S. R., Physics of amorphous materials, 1990.
[2]. https://eic.rsc.org/feature/trouble-in-the-periodic-table/2020266.article (Access Date: 03.03.2019).
[3]. Laurent C., Chalcogenide glasses and glass–ceramics: Transparent materials in the infrared for dual applications, Elsevier, 2016.
[4]. Mehta. N., Applications of chalcogenide glasses in electronics and optoelectronics: A review, J. of Sci. & Ind. Res., 2006, 65: 777–786.
[5]. Shultz–Sellack C., Ann. Phys., 1870, 139: 182.
[6]. Wood R. W., Phil, M., Absorption, dispersion, and surface colour of selenium, 3, 607, 1902.
[7]. Meier W., Ann. Phys., 1910, 31: 1017.
[8]. Frerichs R., Phys. Rev., 1950, 78: 643.
[9]. Frerichs R., J., Opt. Soc. Am., 1953, 43: 1153.
[10]. Fraser W. A. J., Opt. Soc. Am., 1953, 43: 823.
[11]. Dewulf G., Rev. Opt. 1954, 33: 513.

[12]. Winter K. A., Verres et refractaires, 1955, 9: 147.
[13]. Goriunova N. A., Kolomiets B. T., Zhurnal Tekhnicheskoi Fiziki, 1955, 25: 2069.
[14]. Ovshinsky S. R., Phys. Rev. Lett., 1968, 21: 1450.
[15]. Ovshinsky S. R., J. Non–Cryst. Solids, 1970, 2: 99.
[16]. Mott, N. F., Davis E. A., Electronic processes in the non–crystalline materials, Oxford: Clarendon Press, 1979.
[17]. Paul A., Chemistry of glasses, Kluwer Academic, 1999.
[18]. Zallan R., The physics of amorphous solids, John Wiley, New York, 1983.
[19]. Popescu M., Non–cyrstalline chalcogenides, Kluwer Academic, 2000.
[20]. Gill W. D., Street G. B., J. Non–Cryst. Solids, 1973/1974, 13: 120.
[21]. Sarrach J., de Neufiville J. P., Hawoth W. L., J. Non–Cryst. Solids, 1976, 22: 245.
[22]. Hawes L., Nature, 1963, 198: 1267.
[23]. Li D. T., Sharma R. C., Chang Y. A., Bulletin Alloy Phase Diagrams, 1989, 10: 348.
[24]. Abrikosov, N. Kh., Bankina, V. F. et al., Semiconducting II–VI, IV–VI and V–VI compounds, Plenum Press, New York, 1969.
[25]. Chun–Hua L., Pashinkin A. S., Novoselova A. V., Dokl. Acad. Nauk SSSR, 1962, 146(5): 1092.
[26]. Kislitskaya E. A., Nosov V. B., Kokorina V. F., Fiz. Khim. Stekla, 1977, 3(6): 624.
[27]. Tronc P., Bensonssan M., Brenac A., Cebenne C., Phys. Rev. B. 1973, 15: 1.
[28]. Suvorova L. et al., Izv. Acad. Nauk. SSSR. Neorg. Mater., 1974, 10(3): 441.
[29]. Vinogradova G. Z., Dembovskii S. A., Luzhnaya N. P., Zh. Neorg. Khim., 1968, 13(5): 1444.
[30]. Nemilov S. V., Zh. Perikl. Khim., 1964, 37(7): 1452.
[31]. Nemilov S. V., Zh. Perikl. Khim., 1964, 37(8): 1699.
[32]. Zallan R., The physics of amorphous solids, John Wiley, New York, 1983.
[33]. Pazin A. V, Obraztsov A. A. And Borisova Z. U., Izv. Acad. Nauk SSSR. Neorg. Mater., 1972, 8(2): 247.
[34]. Flaschen S. S., Pearson, A. D., Northover W. R., J. Am. Ceram. Soc., 1959, 42(9): 450.
[35]. Flaschen S. S., Pearson, A. D., Northover W. R., J. Am. Ceram. Soc., 1960, 43(5): 274.
[36]. Ligero R. A., Casas–Ruiz M., Vazquez J., Jimenez–Garay R., Phys. and Chem. of Glasses, 1993, 34(1): 12.
[37]. Flaschen S. S., Pearson A. D., Northover W. R. J., Appl. Phys. 1960, 31(1): 219.
[38]. Saffarini G., Appl. Phys. A: Mater. Sci. and Proc., 2002, 74(2): 283.
[39]. Spesr W. E., Lecombor P. J., Phil. Mag., 1976, 33: 935.
[40]. Paul W., Lewis, A. J., et al., Solid State Commun., 1976, 20: 969.
[41]. Araki M., Zaki, H., Solid State Commun., 1976, 18: 1603.
[42]. Ovshinsky, S. R., Amorphous and liquid semiconductors, Ed. Spear, W. E., (Proc. 7th Int. Conf. on Amor. and Liq. Semiconductors, Edinburg), 519, 1977.
[43]. https://www.us.schott.com/advanced_optics/english/products/optical-materials/ir-materials/infrared-chalcogenide-glasses/index.html (Access Date: 06.05.18).
[44]. Zachariasen W. H., J. Am. Ceram. Soc., 1932, 54: 3841.
[45]. Elliott S. R., J. Non–Cryst. Solids, 1986, 81: 71.
[46]. Colomban P., Corset J. (eds.) in Special Issue, J. Raman Spect., 1999.
[47]. Weber W. H., Merlin R. (eds.), Raman scattering in materials science, Springer, New York, 2000.
[48]. Schulte A., Richardson K. A., In near–infrared raman spectroscopy of chalcogenide glasses for integrated optics, recent research developments in non–crystalline solids, Transworld Research Network, Kerala, India, 2001.
[49]. Richardson K., Cardinal T., Richardson M., Schulte A., Seal S., in Engineering glassy chalcogenide materials for integrated optics applications, Wiley–VCH, Weinheim 2003.
[50]. Apling A., Leadbetter A. J., Wright A. C., J. Non–Cryst. Solids, 1977, 23: 369.

[51]. Rivero C., Schulte A. et al. In OSA topical meeting on nonlinear guided waves, Cleanwater, F. L., 2001.
[52]. Schulte A., Rivero C. et al., Opt. Commun., 2001, 198: 125.
[53]. Rivero C., Sharek P. et al., Thin Solid Films, 2003, 425: 59.
[54]. Rivero C. A., Sharek P. S. et al., Proc. Soc. Photo. Opt. Instrum. Eng., 2001, 4468: 47.
[55]. Seal S., Richardson K. A. et al., Phys. Chem. Glasses, 2002, 43: 59.
[56]. Asal R., Rivers P. E., Rutt H. N., J. Phys. Condens. Mater., 1997, 9: 6217.
[57]. Benazeth S., Tuilier M. H. et al., J. Non–Cryst. Solids, 1989, 110: 89.
[58]. G. Lucazeau, S. Barnier, A.M. Loireau–Lozac'h, Mater. Res. Bull., 1977, 12: 437.
[59]. Patnaik P., Handbook of inorganic chemicals, McGraw–Hill, New York, 2003.
[60]. Popescu M. A., Non–crystalline chalcogenides in: Carley LR, Declerck G, Klaassen F. M., Eds. Solid–State Science and Technology Library, Vol 8. Orlando, USA: Kluwer Academic Publishers, 2002.
[61]. Müller U., Inorganic structural chemistry, John Wiley & Sons, West Sussex, England, 2006.
[62]. Weiss J., Mitteilung über interchalkogenverbindungen, IV. Röntgenographische Untersuchungen an Mischkristallen der Zusammensetzung SenS8–n, Z. Anorg. Allg. Chem., 435: 113, 1977.
[63]. Boudreau R. A., Haendler H. M., J. Solid State Chem., 36: 289, 1981.
[64]. Boctor N. Z., Kullerud G., J. Solid State Chem., 1987, 71: 513.
[65]. Eifert J. R., Peretti E. A., The phase diagram of the system tellurium/arsenic, J. Mater. Science, 1968, 3: 293.
[66]. Popov A., In: Fairman, R, Ushkov, B., Eds., Semiconducting chalcogenide glass I, Chapt. 2, Elsevier, Amsterdam, The Netherlands, 2004.
[67]. Kaplow R., Rowe T. A., Averbach B, L. Atomic arrangement in vitreous selenium, Phys. Rev., 1968, 168: 1068.
[68]. Salmon P. S., Martin R. A., Mason, P. E. et al., Nature, 2005, 435: 75.
[69]. Bureau B., Troles J., Le Floch M., et al., Solid State Sci., 2003, 5: 219.
[70]. Mott N. F., Davis E. A., Electron processes in non–crystalline materials, Clarendon Press, Oxford, 1979.
[71]. Nemanich R. J., Galeener F. L., Jr. Mikkelsen J. C. et al., Physica, 1983, 117B–118B: 959.
[72]. Gonçalves A. P., Lopes, E. B., Delaizir G, et al., J. Solid State Chem., 2012, 193: 26.
[73]. Depinna S. P., Cavenett B. C., Phys. Rev. Lett., 1982, 48: 556.
[74]. Tanaka K., Shimakawa K., Amorphous chalcogenide semiconductors and related materials, Springer, New York, 2011.
[75]. Kastner M., Phys. Rev. Lett., 1972, 28: 355.
[76]. Fritzsche H., J. Non–Cryst. Solids, 1971, 6: 49.
[77]. Street R. A., Mott N, F., Phys. Rev. Lett., 1975, 35: 1293.
[78]. Kastner M., Adler D., Fritzsche H., Phys. Rev. Lett., 1976, 37: 1504.
[79]. Tanaka K., Gotoh T., Yoshida N., Nonomura S., J. of Appl. Phys., 2002, 91: 125.
[80]. Boolchand P., Georgiev D. G., Goodman B., J. Optoelectron Mater., 2001, 3(3): 703–720.
[81]. Redaelli A, Pirovano A. et al., IEEE Electron Device Letters, 2004, 25: 648–686.
[82]. Boolchand P., Georgiev D. G. and Goodman B., J. Optoelectron Mater., 2001, 3(3): 703–720.
[83]. Hilton, A. R., Chalcogenide glasses for infrared optics, McGraw A. Ray Hill Companies, 2010.
[84]. Mott N. F., Adv. in Phys., 1967, 16: 49–57, 1967.
[85]. Anderson P. W., Phys. Rev., 1958, 109: 1492.
[86]. Tan, W. C., "Optical properties of amorphous selenium films", PhD thesis, Saskatchewan Univ., 2006.
[87]. Cohen M. H., Fritzsche H. and Ovshinski S. R., Phys. Rev. Lett., 1969, 22: 1065–1072.
[88]. Marshall J. M. and Owen A. E., Philosophical Magazine, 1971, 24: 1281–1290.
[89]. Emin, D., Phys. Rev. Lett., 1970, 25: 1751–1755.

[90]. Tanaka K., Rev. of Solid State Sci., 1990, 4(2 & 3): 511.
[91]. Pfeiffer G., Paesler M. A., Agarwal S. C., J. Non–Cryst. Solids, 1991, 130: 111.
[92]. Tichy L., Ticha H., Nagels P., Callaerts R., J. of Non–Crys. Solids, 1998, 240: 177.
[93]. Lyubin V. M. and Tikhomirov V. K., J. of Non–Crys. Solids, 1991, 135: 37.
[94]. Popescu M., J. of Optoelectronics and Adv. Mater., 2005, 7: 2189–2210.
[95]. Turpin G. B., McNeil L. E., Phys. Rev. B, 1989, 39: 8750.
[96]. Ducharme S., J Hautala J. and Taylor, P. C., Phys. Rev. B, 1990, 41: 12250–12261.
[97]. Othman A. A., Amer H. H., Osman M. A., Dahshan A., Radiation Effects & Defects in Solids, 2004, 159: 659–666.
[98]. Štábl M., Tichi L., Solid State Sci., 2005, 7: 201–207.
[99]. Street R. A., Adv. in Phys., 1976, 25: 397–454.
[100]. Fairman R. and Ushkov B., Semiconducting chalcogenide glass 1, Elsevier Academic Press, Netherlands, 2004.
[101]. Seki M., Hachiya K., Yoshida K., J. of Non–Crys. Solids, 2003, 324: 127–132.
[102]. Akoi T., Komedoori S. et al., J. of Non–Crys. Solids, 2003, 326: 273–278.
[103]. Bishop S. G., Mitchell D. L., Phys. Rev. B, 1973, 8: 5696–5701.
[104]. Zakery A., Elliott S. R., Optical nonlinearities in chalcogenide glasses and their applications, Springer–Verlag Berlin, Heidelberg, 2007.
[105]. Sanghera J. S., Florea C. M. et al., J. of Non–Crys. Solids, 2008, 354: 462–467.
[106]. Ganeev R. A., Ryasnyanski A. I., Usmanov T., Phys. of the Solid State, 2003, 45: 207–213.
[107]. Ganeev R. A., Ryasnyansky A, Kodirov M. K., Usmanov T., J. Opt. A: Pure Appl. Opt., 2002, 4: 446–451.
[108]. Nasu H., Kubodera K. I. et al., J. Am. Ceram. Soc., 1990, 73: 1794–1796.
[109]. Borisova Z., Glassy semiconductors, Plenum Press, New York, 1981.
[110]. Shiryaev V. S., Churbanov M. F., "Chap. 1, Chalcogenide glasses: preparation, properties and applications in: Adam J. L, Zhang X., Eds. Woodhead Publishing, 2014.
[111]. Feltz A., Amorphous inorganic materials and glasses, Weinheim: VCH Verlag, 1993.
[112]. Inagawa I., Iizuka R., Yamagishi T., et al., J. Non–Cryst. Solids, 1987, 95–96: 801.
[113]. Piarristeguy A. A., Barthélémy E., Krbal M., et al. J. Non–Cryst. Solids, 2009, 355: 2088.
[114]. Shiryaev V. S., Ketkova L. A., Churbanov M. F. et al., J. of Non–Cryst. Solids, 2009, 355: 2640.
[115]. Pradel A., Ribes M., Solid State Ionics, 1986, 18–19: 351.
[116]. Hayashi A., Minami K., Tatsumisago M., J. Solid State Electrochem., 2010, 14: 1761.
[117]. Hubert M., Delaizir G., Monnier J. et al., Opt. Exp., 2011, 19(23): 23513.
[118]. Orava J., Kohoutek T., Wagner T., In Adam J. L., Zhang X. H., Eds., Chalcogenide glasses: Preparation, properties and applications, Chap. 9, Woodhead Publishing, 2014.
[119]. Belev G., Kasap S., Rowlands J., et al., Curr. Appl. Phys., 2008, 8: 383.
[120]. Kahnt H., Feltz A., Thin Solid Films, 1982, 98: 211.
[121]. Simpson R. E., Krbal M., Fons P., et al., Nano–letters, 2010, 10: 414.
[122]. Nazabal V., Nemec P., Jedelsky J., et al., Opt. Mater., 2006, 29: 273.
[123]. Kloock J. P., Mourzina Y. G., Schuberg J. et al., Sensors, 2002, 2; 356.
[124]. Curry R., Mairaj A., Huang C., et al., J. Am. Ceram. Soc., 2005, 88: 2451.
[125]. Chern G., Lauks I., J. Appl. Phys., 1982, 53: 6979.
[126]. Street R. A. and Mott N. F., Phys. Rev. Letters, 1975, 35: 1293.
[127]. Ganeev R. A., Ryasnyansky A., Kodirov M. K. and Usmanov T., J. Opt. A: Pure Appl. Opt., 2002, 4: 446–451.
[128]. Andriesh A. M., Ponomar V. V. et al., Sov. J. Quantum Electron, 1986, 16(6): 721–736.
[129]. Andriesh A., J. of Optoelec. and Adv. Mater., 2005, 7: 2931–2939.
[130]. Lezal D., J. of Optoelectronics and Adv. Mater., 2003, 5: 23–34.
[131]. Sanghera J. S. and Aggarwal I. D., J. of Non–Cryst. Solids, 190, 2573(6): 1794.

[132]. Adam J.–L. and Zhang X., Chalcogenide glasses preparation, properties and applications, 2014.
[133]. Michel K., Bureau B., Boussard–Plédel C., et al., Sensors and Actuators B, 2004, 101: 252.
[134]. Wilhelm A., Boussard–Plédel C., Coulombier Q., et al., Adv. Mater., 2007, 19(22): 3796.
[135]. Lucas P., LeCoq D., Juncker C., et al., Appl. Spectr., 2005, 59: 1.
[136]. Brandily M. L., Monbet V., Bureau B., et al., Sensors and Actuators B: Chemical, 2011, 160(1): 202.
[137]. Tatsumisago M, Hayashi A., Solid State Ionics, 2012, 225: 342.
[138]. Mori K., Ichida T., Iwase K., et al., Chem. Phys. Letters, 2013, 584: 113.
[139]. Urena A., Piarristeguy A. et al. J. of Phys. and Chem. of Solids, 2007, 68: 993–997.
[140]. Balan V., Vigreux C., Pradel A., J. of Optoelectronics and Adv. Mater., 2004, 6, 875–882.
[141]. Huang C. C., Heak D. W., Electronic Letters, 2004, 40: 863–865.
[142]. Tintu R., Nampoori V. P. N. et al., Optics Commun., 2011, 284: 222–225.
[143]. Márquez E., Bernal–Oliva A. M. et al., J. of Non–Crys. Solids, 1997, 222: 250.
[144]. Siemann U., Progr. Colloid. Polym. Sci., 2005, 130: 1–14.
[145]. Litty I., Deepthy A. et al., J. of App. Phys., 2008, 103: 033105.
[146]. Litty I., Deepthy A. et al., J. of Appl. Phys., 2007, 102: 063524.
[147]. Litty I., L. Bindu K. et al., J. of Phys. D: Appl. Phys., 2007, 40: 5670–5674.
[148]. Litty I., Dann V. J. et al., Laser Phys., 2008, 18(7): 882–885.
[149]. Tintu R., Nampoori V. P. N. et al., J. of App. Phys., 2010, 108: 073525.
[150]. Ganeeva R. A., Ryasnyansky I., Usmanov T., Optical and Quantum Electronics, 2003, 35: 211–219.
[151]. Berzelius J. J., Ann. Chim. Phys., 1826, 32: 166. (2) Bineau A., Ann. Chim. Phys., 1839, 70: 54.
[152]. Kohoutek T., Wagner T. et al., J. of App. Phys., 2008, 103: 063511.
[153]. Shtutina S., Klebanov M., Lyubin S. R. V., Volterra V., Thin Solid Films, 1995, 261: 263–265.
[154]. Mamedov S. B., Michailov M. D., J. of Non–Crys. Solids, 1997, 221: 181–186.
[155]. Michailov M. D., Mamedov S. B., Tsventarnyi S. V., J. of Non–Crys. Solids, 1994, 176: 258–262.
[156]. Orava J., Wagner T. et al., J. of Non–Crys. Solids, 2006, 352: 1637–1640.
[157]. Song S., Carlie N. et al., J. of Non–Crys. Solids, 2009, 355: 2272–2278.
[158]. Chern G. C. and Lauks I., J. of App. Phys., 1982, 53(10): 6979.
[159]. Chern G. C., Lauks I., McGhie A. R., J. of App. Phys., 1983, 54(8): 4596.
[160]. Chern G. C., Lauks I., J. of App. Phys., 1983, 54: 2701.
[161]. Carlie N. A., A Solution–based approach to the fabrication of novel chalcogenide glass materials and structures, PhD thesis, Clemson Univ., 2010.
[162]. Song S., S. Howard S. et al., Appl. Phys. Letters, 2006, 89(4): 041115.
[163]. Kohoutek T., Orava J., Sawada T., Fudouzi H., J. of Colloid and Interface Sci., 2011, 353: 454–458.
[164]. Kim S. H. and Hwangbo C. K., Opt. Letters, 1998, 23: 1573–1575.
[165]. Kohoutek T., Orava J. et al., J. Phys. Chem. Solids, 2007, 68: 2376–2380.
[166]. Balan V., Vigreux C. et al., J. of Optoelectronics and Adv. Mater., 2001, 3: 367–372.
[167]. Kohoutek T., Wagner T. et al., J. of Non–Crys. Solids, 2008, 354: 529–532.
[168]. Kim S. H. and Hwangbo C. K., Appl. Opt., 2002, 41: 3187–3192.
[169]. DeCorby R. G., Nguyen H. T. et al., 2005, 13: 6228–6233.
[170]. DeCorby R. G., Ponnampalam N. et al., IEEE J. Sel. Top. Quantum Electron, 2005, 11: 539–546.
[171]. Clement T. J., Ponnampalam N. et al., Opt. Exp., 2006, 14: 1789.
[172]. Bormashenko E., Pogreb R., Pogreb Z. and Semion Sutovski S., Opt. Eng., 2001, 40: 661.
[173]. Andriesh A. and Iovu M., Phys. Status Solidi B, 2009, 246: 1862–1865.
[174]. Bendow B., Rast H. & El–Bayoumi O. H., Opt. Eng., 1985, 24(6): 1072–1078.

[175]. Klocek P., Roth M. & Rock R. D., Opt. Eng., 1987, 26(2): 88.
[176]. Troles J., Coulombier Q. et al., Opt. Exp., 2010, 18(25): 26647–26654.
[177]. El–Amraoui M., Gadret G. et al., Opt. Express, 2010, 18(25): 26655–26665.
[178]. Weiblen R. J., Docherty A., Hu J. and Menyuk C. R., Opt. Express, 2010, 1 (25): 26666–26674.
[179]. Seddon A. B., Tang Z. et al., Opt. Express, 2010, 18(25): 26704–26719.
[180]. Mori A., Ohishi Y., Kanamori T. and Sudo S., App. Phys. Letters, 1997, 70: 1230.
[181]. Kim J., Paek U–C. et al., Opt. Letters, 2006, 31: 1196–1198.
[182]. Monro T. M., West Y. D. et al., J, Elec. Lett., 1998, 36.
[183]. Troles J., Brilland L. et al., Fiber and Integ. Opt., 2008, 28: 11–26.
[184]. Jacques L., Johann T., Xiang H. Z., Catherine B. P., Marcel P., Bruno B., Glasses to see beyond visible, Published by Elsevier Masson SAS, 2018, 21: 916-922.
[185]. Birks T. A., Roberts P. J. et al., Elect. Lett. 1995, 31: 1941.
[186]. Trolès J., Brilland L., Caillaud C., Adam J. L., Adv. Device Mater., 2017, 1.
[187]. Petersen C. R., Engelsholm R. D. et al., Opt. Exp., 2017, 25: 15336.
[188]. Toupin P., Brilland L. et al., J. Non–Cryst. Solids, 2013, 377: 217–219.
[189]. Trolès J., Brilland L., Chalcogenide microstructured optical fibres for mid–IR applications, Published by Elsevier Masson SAS, 2017, 18: 19–23.
[190]. Trolès J., Coulombier Q. et al. Opt. Exp., 2010, 18: 26647–26654.
[191]. Toupin P., Brilland L. et al. Opt. Mater. Exp., 2, 2012, 1359–1366.
[192]. Caillaud C., Gilles C. et al., Opt. Exp., 2016, 24: 7977–7986.